

Investigating macroscopic quantum superpositions and the quantum-to-classical transition by optical parametric amplification

Francesco De Martini*

*Dipartimento di Fisica, Sapienza Università di Roma, Italy and
Accademia dei Lincei, via della Lungara 10, I-00165 Roma, Italy*

Fabio Sciarrino†

Dipartimento di Fisica, Sapienza Università di Roma, I-00185 Roma, Italy

The present work reports on an extended research endeavor focused on the theoretical and experimental realization of a macroscopic quantum superposition (MQS) made up with photons. As it is well known, this intriguing, fundamental quantum condition is at the core of a famous argument conceived by Erwin Schroedinger, back in 1935. The main experimental challenge to the actual realization of this object resides generally on the unavoidable and uncontrolled interactions with the environment, i.e. the "decoherence" leading to the cancellation of any evidence of the quantum features associated with the macroscopic system. The present scheme is based on a nonlinear process, the "quantum injected optical parametric amplification", that maps by a linearized cloning process the quantum coherence of a single - particle state, i.e. a Micro - qubit, into a Macro - qubit, consisting in a large number M of photons in quantum superposition. Since the adopted scheme was found resilient to decoherence, the MQS demonstration was carried out experimentally at room temperature with $M \geq 10^4$. This result elicited an extended study on quantum cloning, quantum amplification and quantum decoherence. The related theory is outlined in the article where several experiments are reviewed such as the test on the "no-signaling theorem" and the dynamical interaction of the photon MQS with a Bose-Einstein condensate. In addition, the consideration of the Micro - Macro entanglement regime is extended into the Macro - Macro condition. The MQS interference patterns for large M were revealed in the experiment and the bipartite Micro-Macro entanglement was also demonstrated for a limited number of generated particles: $M \lesssim 12$. At last, the perspectives opened by this new method are considered in the view of further studies on quantum foundations and quantum measurement.

Contents			
I. INTRODUCTION	2	2. Pseudo-spin operators	13
II. OPTICAL PARAMETRIC AMPLIFICATION	3	3. Correlation measurements via orthogonality filter	14
A. Non-collinear amplifier	4	4. Effects of coarse-grained measurement	15
B. Collinear amplifier	5	5. Hybrid criteria	15
III. OPTIMAL QUANTUM MACHINES VIA PARAMETRIC AMPLIFICATION	6	VII. RESILIENCE TO DECOHERENCE OF THE AMPLIFIED MULTIPARTICLE STATE	15
A. Universal optimal quantum cloning	7	A. Phase-covariant optimal quantum cloning machine	16
B. Universal optimal NOT gate	8	B. Universal optimal quantum cloning machine	16
C. Optimal machines by symmetrization	9	C. Effective size of the multiparticle superposition	17
D. Phase-covariant optimal quantum cloning	9	VIII. WIGNER - FUNCTION THEORY	18
IV. PARAMETRIC AMPLIFICATION AND NO-SIGNALING THEOREM	10	IX. GENERATION OF MACRO-MACRO ENTANGLED STATES	18
V. EXPERIMENTAL MACROSCOPIC QUANTUM SUPERPOSITION BY MULTIPLE CLONING OF SINGLE PHOTON STATES	11	A. Macroscopic quantum state based on high gain spontaneous parametric down-conversion	19
A. Generation and detection of multi-particle quantum superpositions	11	1. Non-separable Werner states	20
VI. MICRO-MACRO SYSTEM: HOW TO DEMONSTRATE ENTANGLEMENT	13	2. Quantum-to-classical transition by dichotomic measurement	20
1. Extracted two photon density matrices	13	B. Macroscopic quantum state by dual amplification of two-photon entangled state	21
		X. INTERACTION WITH A BOSE-EINSTEIN CONDENSATE	21
		XI. APPLICATIONS: FROM SENSING TO RADIOMETRY	22
		A. Quantum sensing	22
		B. Quantum radiometry	23
		XII. CONCLUSIONS AND PERSPECTIVES	23
		Acknowledgments	24

*Electronic address: francesco.demartini@uniroma1.it

†Electronic address: fabio.sciarrino@uniroma1.it

I. INTRODUCTION

Since the golden years of quantum mechanics (Schrödinger, 1935) the possibility to observe the quantum features of physical systems at the macroscopic level has been the object of extensive theoretical studies and recognized as a major conceptual paradigm of physics. However, in general severe problems stand up to spoil the observation of these features. As it is well known, the most important one is the unavoidable interaction with the surrounding environment that determines the loss of any quantum coherence effect by the corruption of the phase implied by any correlation of the quantum states (Zurek, 2003). Such effects are commonly believed to become increasingly severe with the growing of the size of the system being studied (Raimond *et al.*, 2001).

In the last several years many experimental attempts have been undertaken to create superposition of multiparticle quantum states. Different experimental approaches have been pursued based on atom-photon interacting in a cavity (Haroche, 2003; Raimond *et al.*, 2001), superconducting quantum circuits (Leggett, 2002), ions (Leibfried *et al.*, 2003), micromechanical systems (Marshall *et al.*, 2003), optical systems (Ourjoumtsev *et al.*, 2006, 2007). In particular in the last few years a significant advance toward generating superposition states of large objects using optomechanical systems has been achieved (Groblacher *et al.*, 2004; Rocheleau *et al.*, 2004; Teufel *et al.*, 2011). When dealing with the superposition of multiparticle quantum states, two are the fundamental issues to be considered: what is the effective size of the superpositions and how the state behaves under decoherence phenomena (Leggett, 2002). Several criteria have been developed to establish the effective size of macroscopic superpositions in interacting or imperfect scenario, as well as their applications to real systems (Dur *et al.*, 2002; Korsbakken *et al.*, 2007; Leggett, 2002). A large effective size of the state usually conflicts with the robustness of the quantum superposition under interaction with environment. Moreover the observation of macroscopic interference phenomena requires to tailor proper measurement strategies. In particular one faces the problem of achieving a measurement-precision that enables the observation of quantum effects at such macro-scales (Kofler and Brukner, 2007).

In this paper we discuss how the amplification of quantum states can be adopted to generate multiphoton superpositions and to investigate the quantum-to-classical transition. By the present method a quantum superposition state is first generated in the microscopic (Micro) world of a single photon particle. Then, such system is mapped into the macroscopic (Macro) realm by generating a quantum superpositions via the well known "photon stimulation" process of quantum electrodynamic

(QED) in the regime of high gain parametric amplification (De Martini, 1998a,b). Such approach is a natural platform for the investigation of the quantum-to-classical transition, linking quantum and classical matter description. We will review the properties of the generated states both in the regime of low and high number of photons. The experimental methods will be outlined and the corresponding results reported and briefly described. The open question to devise a method apt to demonstrate experimentally the Micro-Macro entanglement will be finally addressed.

Let's first consider the regime in which few particles are created by optical amplification of a single photon in the generic polarization state: $|\phi\rangle = \alpha|H\rangle + \beta|V\rangle$, where H and V stand for the horizontal and vertical polarization, respectively. This process can be related to several fundamental tasks of quantum information processing. While classical information is represented in terms of bits which can be either 0 or 1, the quantum information theory is rooted on the generation and transformation of quantum-bits, or qubits, which are two-dimensional quantum systems, each epitomized by a spins- $\frac{1}{2}$ (Nielsen and Chuang, 2000). A qubit, unlike a classical bit, can exist in a state $|\phi\rangle$ that is a superposition of any couple of orthogonal basis states $\{|0\rangle, |1\rangle\}$, i.e., $|\phi\rangle = \alpha|0\rangle + \beta|1\rangle$. The fact that qubits can exist in superposition states gives to quantum information unusual properties. For instance, a fundamental issue refers to the basic limitations imposed by quantum mechanics to the set of realizable physical transformations imposed to the state of any quantum system. The common denominator of these bounds is that all realizable transformations have to be represented by completely positive maps which in turn impose a constraint on the "fidelity", i.e., the quantum efficiency, of the quantum measurements. For instance, the fact that an unknown qubit cannot be precisely determined (or reconstructed) by a measurement performed on a finite ensemble of identically prepared qubits implies that this state "cannot be cloned", viz. copied exactly by a general transformation. In other words, the "universal", exact cloning map of the form $|\phi\rangle \rightarrow |\phi\rangle|\phi\rangle$, or more generally where N are cloned into $M > N$ copies, is not allowed by the quantum mechanics rules (Wootters and Zurek, 1982). Indeed, if this were possible then one would be able to violate the bound on the fidelity of estimation and this in turn would trigger most dramatic changes in the present picture of the physical world. For instance, it would become possible to exploit the non-local quantum correlations for superluminal exchange of meaningful information, by then violating the causality principle (De Angelis *et al.*, 2007; Herbert, 1982). Another map which cannot be performed exactly on an unknown qubit is the "spin-flip", generally dubbed "Universal-NOT" transformation. This corresponds to the operation $|\phi\rangle \rightarrow |\phi^\perp\rangle$, where the state $|\phi^\perp\rangle$ is orthogonal to the original $|\phi\rangle$ (Bechmann-Pasquinucci and Gisin, 1999; De Martini *et al.*, 2002). The quantum cloning and the NOT maps are just two amongst a large variety of ex-

amples realizing the effects of the essential limitations imposed by quantum mechanics on measurements and estimations.

In spite of the fact that these quantum-mechanical transformations on unknown qubits cannot be performed "exactly", one still may ask what are the best possible, i.e. "optimal", approximations of these maps within the given structure of quantum theory (Cerf and Fiurasek, 2006; De Martini and Sciarrino, 2005; Scarani *et al.*, 2005). In the last few years, it was found possible to associate an optimal cloning machine with a photon amplification process, e.g. involving inverted atoms in a laser amplifier or a nonlinear medium in a "quantum-injected" (QI) "optical parametric amplifier" (OPA) apparatus, dubbed (QI-OPA) (De Martini *et al.*, 2000; Simon *et al.*, 2000). In the case of the mode non degenerate QI-OPA, N photons, prepared identically in an arbitrary quantum state $|\phi\rangle$ of polarization are injected into the amplifier. By stimulated emission $M - N$ pairs of photons are created. On the output of the amplifier generates, in the "cloning mode" are found $M > N$ copies are, or "clones" of the input qubit $|\phi\rangle$ (De Martini *et al.*, 2002, 2004; Lamas-Linares *et al.*, 2002). Correspondingly, the amplifier generates on the output "anticloning mode", $M - N$ states $|\phi^\perp\rangle$, thus realizing an universal quantum NOT gate (De Martini *et al.*, 2002). Moreover the optimal quantum cloning turns out be tightly connected with the no-signaling condition (Gisin, 1998).

Let us now address the regime in which a large number of particles is generated by the amplification process of a single photon in a quantum superposition state of polarization. Conceptually, the method consists of transferring the well accessible condition of quantum superposition of a one photon qubit to a mesoscopic, i.e., multiphoton amplified state $M > 1$, here referred to as a "mesoscopic qubit", or "Macro-qubit". This can be done by injecting in the QI-OPA the one photon qubit $\alpha|H\rangle + \beta|V\rangle$ (De Martini, 1998a; De Martini *et al.*, 2005, 2009a). This process is represented in Figure 1 which shows three possible schematic applications of the method. In virtue of the "information preserving" (albeit "noisy") property of the amplifier, the generated state is found to keep the same superposition character and the interfering properties of the injected qubit. Since the adopted scheme realizes the optimal quantum cloning machine, able to copy optimally any unknown input qubit into copies with optimal fidelity, the output state will be necessarily affected by squeezed-vacuum noise arising from the input vacuum field. We will review the properties of such Macro states obtained by the quantum injected amplification process and how they can be exploited to investigate entanglement in the microscopic-macroscopic (Micro-Macro) regime. Precisely, there an entangled photon pair is created by a nonlinear optical process; then one photon of the pair is injected into an optical parametric amplifier operating for any input polarization state (De Martini *et al.*, 2009a, 2008). Such

transformation establishes a connection between the single photon and the multiparticle fields. The results of a thorough theoretical analysis undertaken on this process will be outlined. The results of a series of related experiments will be reported. We shall show that while a clear experimental evidence of a MQS interference, in absence of bipartite Micro-Macro entanglement, has been attained with a fairly large associated number M of particles, the Micro-Macro entanglement could be consistently demonstrated, by an attenuation technique only for a small number of particles: $M \leq 12$. Indeed, as suggested by (Sekatski *et al.*, 2009; Spagnolo *et al.*, 2010c) a novel "detection loophole" for large M and the need of very high measurement resolution impose severe limitations to the detection of quantum entanglement in the Micro-Macro regime, i.e. of the prerequisite condition for the full realization of the Schrödinger Cat program. In addition, we shall briefly summarize the potential applications of the QI-OPA technique in different contexts, such as the realization of a non-locality test, quantum metrology and quantum sensing.

At last we shall consider a further approach to investigate the quantum-to-classical transition based on nonlinear parametric interactions, i.e. the one that exploits the process of spontaneous parametric down-conversion (SPDC) in the high gain regime. In this framework the investigation of multiphoton states is of fundamental importance, on both conceptual and practical levels, e.g., for nonlocality tests or for other quantum information applications. The number of photons generated depends exponentially on the nonlinear gain g of the parametric process where g can be increased by the adoption of high-power pumping lasers and high-efficiency non-linear crystals. Different experimental approaches to generate Macro-Macro entangled states and to observe non-local correlations will be reviewed (Caminati *et al.*, 2006a; De Martini, 2010; Eisenberg *et al.*, 2004; Vitelli *et al.*, 2010c). Again the issue of high-resolution measurements will arise as a fundamental ingredient to directly observe quantum correlations in the macroscopic regime.

II. OPTICAL PARAMETRIC AMPLIFICATION

Let us now introduce the non-degenerate optical parametric amplifier which lies at the core of the present analysis. Consider Figure 1 a). Three different modes of the electromagnetic radiation field - say the signal \hat{a}_1 , the idler \hat{a}_2 and the pump \hat{a}_P - are coupled by a non-linear (NL) medium, generally a crystal, characterized by a high third-order tensor expressing the nonlinear "second-order susceptibility" $\chi^{(2)}$ (Boyd, 2008; Walls and Milburn, 1995; Yariv, 1989). A typical NL medium, adopted in the experiments dealt with in this article, consists of a suitably cut slab of crystalline *beta barium borate*, commonly dubbed (BBO). Two "phase matching" conditions must be fulfilled during the coherent three-wave interaction, viz. a scalar one, the energy

conservation, and a vectorial one, the momentum conservation:

$$\nu_P = \nu_1 + \nu_2 \quad (1)$$

$$\vec{k}_P = \vec{k}_1 + \vec{k}_2 \quad (2)$$

where the labels $\{P, 1, 2\}$ refer to the "pump", signal and idler field modes, respectively. The Hamiltonian of the amplifier under the phase-matched condition (2) can be written in the rotating wave approximation as follows

$$\hat{\mathcal{H}} = ik\hbar \left(\hat{a}_1^\dagger \hat{a}_2^\dagger \hat{a}_P + \hat{a}_1 \hat{a}_2 \hat{a}_P^\dagger \right) \quad (3)$$

The first term of the Hamiltonian (3) describes the physical process in which a photon is annihilated at frequency ν_P and the twin photons are generated at frequencies ν_1 and ν_2 . The second term corresponds to the inverse process. In exact phase-matching condition the parameter k is proportional to the crystal $\chi^{(2)}$ and to the effective crystal length l_{crist} (Boyd, 2008; Yariv, 1989).

The Hamiltonian in Eq.(3) describes also the frequency degenerate case, case in which the frequencies associated with the modes \hat{a}_1 and \hat{a}_2 are equal but the respective wave-vectors and/or polarizations are different. The quantum dynamics determined by the Hamiltonian (3) leads to a rich variety of phenomena, such as generation of strongly correlated photon pairs by parametric down-conversion (Ou and Mandel, 1988; Rarity and Tapster, 1990; Shih and Alley, 1988), quantum-injected optical parametric amplification (De Martini, 1998a) phase insensitive amplification (Mollow and Glauber, 1967), generation of polarization entanglement (Kwiat *et al.*, 1995a). The unitary evolution operator associated with $\hat{\mathcal{H}}$ in the interaction picture is expressed as:

$$\hat{U} = \exp \left[\tau \left(\hat{a}_1^\dagger \hat{a}_2^\dagger \hat{a}_P + \hat{a}_1 \hat{a}_2 \hat{a}_P^\dagger \right) \right] \quad (4)$$

where $\tau = kt$, t being the interaction time.

The pump field \hat{a}_P is well described by a coherent state (the "quasi-classical" Glauber's α -state), generally taken as undepleted because of the small number of converted photons compared with the very large number of photons, typically larger than 10^{15} associated with each pump pulse. A precise Manley-Rowe theory accounting for the pump depletion could be possibly adopted, if necessary. Hence, in the generally adopted "parametric approximation" the pump mode \hat{a}_P is replaced with the complex amplitude of the corresponding coherent state. In that case the interaction Hamiltonian leads to the two-mode squeezing operator (Walls and Milburn, 1995):

$$\hat{S} = \exp \left[\tau \left(\alpha_P \hat{a}_1^\dagger \hat{a}_2^\dagger + \alpha_P^* \hat{a}_1 \hat{a}_2 \right) \right] \quad (5)$$

The operator \hat{S} acting on the vacuum state $|0\rangle_1 |0\rangle_2$ creates, via the process of spontaneous parametric down-conversion (SPDC) the "twin beam state" over the two spatial output modes \mathbf{k}_i ($i = 1, 2$) with wavelength λ_i :

$$\hat{S} |0\rangle_1 |0\rangle_2 = \frac{1}{\cosh \tau} \sum_{n=0}^{\infty} \tau^n |n\rangle_1 |n\rangle_2 \quad (6)$$

The average photon numbers \bar{n} on the two modes are related to the gain $g = |\tau|$ as follows: $\bar{n} = \sinh^2 g$. Let us provide some numerical estimate by considering a commonly adopted apparatus. With a BBO crystal, 1mm thick, $\lambda_P = 400nm$ and $\lambda_1 = \lambda_2 = 800nm$, the efficiency of the SPDC process is very low, typically around 10^{-15} .

In general, the pump field can be either a continuous or a pulsed beam (De Martini and Sciarrino, 2005). Pulsed lasers are used when a high interaction gain and/or an exact knowledge of the creation time of a photon pair (a "biphoton") are requested. When this is the case mode-locked laser beams are adopted with a typical pulse duration of hundreds of femtoseconds. In the SPDC two different types of phase matching (either I or II) are used depending on the polarization of the three interacting fields, i.e. on the character of the corresponding electromagnetic waves in the birefringent non-linear crystal, whether "ordinary wave" (o) or "extraordinary wave" (e). Hereafter we will consider only type II phase-matching, in which signal and idler are respectively o and e polarized. The spatial distribution of the emitted SPDC radiation consists of two \mathbf{k} -vector cones, one for each type of wave, having common vertices coinciding with the excited spot on the NL crystal slab, considered very thin. We will restrict for simplicity to the frequency degenerate case only, i.e. $\nu_1 = \nu_2 = \nu_P/2$. In the case of type II phase matching two different \mathbf{k} -vector cones are emitted, the o -cone and the e -cone having the same vertex, different axes and intersecting along two straight lines. The two \mathbf{k} -vectors, correlated with different polarizations by the type II parametric interaction, are parallel to these intersection lines and belong to different cones. The angle between the axes of these polarization cones can be changed by a convenient tilting of the NL slab with respect to the direction of the "pump" beam. When this angle is zero the two \mathbf{k} -vectors overlap, each one keeping his own polarization. This condition corresponds to the collinear interaction we shall consider shortly, below.

A. Non-collinear amplifier

The interaction Hamiltonian for the type II amplifier in the noncollinear regime is given by $\hat{\mathcal{H}}_U = i\hbar\chi(\hat{a}_{1\psi}^\dagger \hat{a}_{2\psi_\perp}^\dagger - \hat{a}_{1\psi_\perp}^\dagger \hat{a}_{2\psi}^\dagger) + \text{H.c.}$: Figure 1-a). Since this system possesses a complete SU(2) symmetry, the Hamiltonian maintains the same form for any simultaneous rotation of the Bloch sphere of the polarization basis for both output modes \mathbf{k}_1 and \mathbf{k}_2 . Let us now analyze the features of this device when adopted in the stimulated emission by a single photon with polarization $|\psi\rangle$, i.e. in the single - injection QI-OPA regime. The output state of the amplifier reads:

$$|\Phi_U^{1\psi, 0\psi_\perp}\rangle = \hat{U}_U |1\psi\rangle_1 = \frac{1}{C^3} \sum_{n,m=0}^{\infty} \Gamma^{n+m} (-1)^m \sqrt{n+1} | (n+1)\psi, m\psi_\perp \rangle_1 \otimes | m\psi, n\psi_\perp \rangle_2 \quad (7)$$

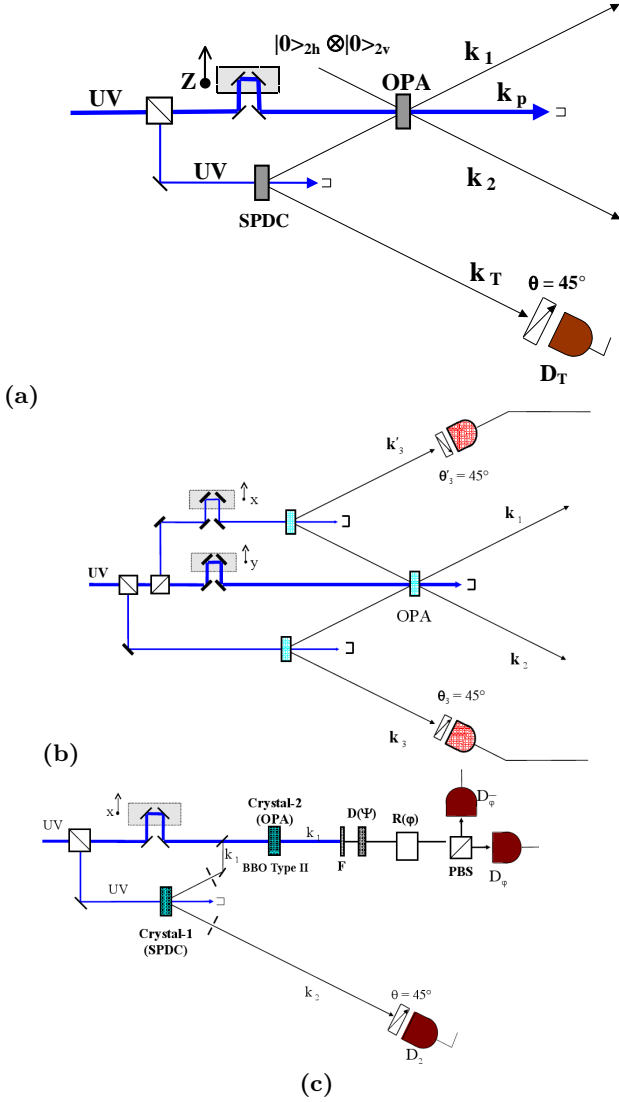


FIG. 1 Three different configurations for the amplification of quantum states. (a) Schematic diagram of the non-collinear quantum injected optical parametric amplifier. The injection is provided by an external spontaneous parametric down conversion source of polarization entangled photon states (De Martini, 1998a). (b) Double-injection of the optical parametric amplifier (Bovino *et al.*, 1999). (c) Collinear quantum injected optical parametric amplifier (De Martini, 1998b).

where $C = \cosh g$, $\Gamma = \tanh g$, and $|p\psi, q\psi_\perp\rangle_i$ stands for a Fock state with p photons polarized $\vec{\pi}_\psi$ and q photons polarized $\vec{\pi}_{\psi_\perp}$ on spatial mode \mathbf{k}_i . Note that the multi-particle states $|\Phi_U^{1\psi}\rangle$, $|\Phi_U^{1\psi_\perp}\rangle$ are orthonormal.

Let us note that previous expression involves superpositions of quantum states with different photon numbers. Clearly the number of photons in the pump beam would change slightly, however the pumping beam is a coherent state with large number of photons hence this variation is negligible and the pumping beam state can be factorized.

Let us analyze the output field \mathbf{k}_1 over the polarization

modes $\vec{\pi}_\pm$ when the state $|\varphi\rangle_1 = 2^{-\frac{1}{2}}(|H\rangle_1 + e^{i\varphi}|V\rangle_1)$ is injected. The average photon number M_\pm^i over \mathbf{k}_i with polarization $\vec{\pi}_\pm$ is found to depend on the phase φ as follows:

$$M_\pm^1(\varphi) = \bar{m} + \frac{1}{2}(\bar{m} + 1)(1 \pm \cos \varphi) \sinh^2 g \quad (8)$$

$$M_\pm^2(\varphi) = \bar{m} + \frac{1}{2}\bar{m}(1 \mp \cos \varphi) \quad (9)$$

with $\bar{m} = \sinh^2 g$. The conditions $\varphi = 0$ and $\varphi = \pi$ correspond to single-photon injection and no-injection on the mode $\vec{\pi}_+$, respectively. The average photon number related to both cases is: $M_+^1(0) = 2\bar{m} + 1$ and $M_+^1(\pi) = \bar{m}$. The average number of photons emitted over the two polarizations over \mathbf{k}_1 is found to be $M = 3\bar{m} + 1$. The output state on mode \mathbf{k}_1 with polarization $\vec{\pi}_\pm$ exhibits a sinusoidal fringe pattern of the field intensity depending on φ with a gain-dependent visibility $\mathcal{V}_U^{th} = \frac{\bar{m}+1}{3\bar{m}+1}$ (De Martini, 1998b). Note that for $g \rightarrow \infty$, viz. $M \rightarrow \infty$ the fringe visibility attains the asymptotic values $\mathcal{V}_U^{th} = (\frac{1}{3})$. The former considerations are valid for any quantum state injected in the amplifier $|\phi\rangle$ when analyzed in the polarization basis $\{\vec{\pi}_\phi, \vec{\pi}_{\phi_\perp}\}$.

A more sophisticated extension of the above scheme is the condition of QI-OPA double-injection represented by Figure 1-b) (Bovino *et al.*, 1999). Two separated SPDC sources of polarization entangled photons are adopted to excite simultaneously over the modes \mathbf{k}_1 and \mathbf{k}_2 the QI-OPA amplifier. Meanwhile, the two photons emitted over the external modes \mathbf{k}_3 and \mathbf{k}'_3 generate, by a coincidence circuit, the overall trigger pulse for the experiment when the *opposite* polarizations are realized simultaneously. Owing to the NL dynamics realized by the main NL crystal, the corresponding qubits injected on the two input QI-OPA modes \mathbf{k}_1 and \mathbf{k}_2 with different polarizations give rise to various dynamical processes within the the QI-OPA amplification. For instance they can lead to an enhanced interference fringe visibility: $\mathcal{V}_U^{th-2} = \frac{2}{3}$.

B. Collinear amplifier

Let us consider now the results obtained for a collinear optical configuration in which the two modes \mathbf{k}_1 and \mathbf{k}_2 are made to overlap: Figure 1-c). The interaction Hamiltonian of this process is: $\hat{\mathcal{H}}_{PC} = i\hbar\chi\hat{a}_H^\dagger\hat{a}_V^\dagger + \text{H.c.}$ in the $\{\vec{\pi}_H, \vec{\pi}_V\}$ polarization basis. The same Hamiltonian is expressed as $\hat{\mathcal{H}}_{PC} = \frac{i\hbar\chi}{2}e^{-i\phi}(\hat{a}_\phi^{\dagger 2} - \hat{a}_{\phi_\perp}^{\dagger 2}) + \text{H.c.}$ for any equatorial basis $\{\vec{\pi}_\phi, \vec{\pi}_{\phi_\perp}\}$ on the Poincaré sphere having as poles the states: $\vec{\pi}_H, \vec{\pi}_V$. The amplified state for an injected equatorial qubit $|\varphi\rangle_1$ is:

$$|\Phi_{PC}^\phi\rangle = \hat{U}_{PC}|1\varphi, 0\varphi_\perp\rangle_1 = \sum_{i,j=0}^{\infty} \gamma_{ij}|(2i+1)\varphi, (2j)\varphi_\perp\rangle_1 \quad (10)$$

where $\gamma_{ij} = \frac{1}{C^2} (e^{-i\varphi} \frac{\Gamma}{2})^i (-e^{-i\varphi} \frac{\Gamma}{2})^j \frac{\sqrt{(2i+1)!} \sqrt{(2j)!}}{i!j!}$, $C = \cosh g$, $\Gamma = \tanh g$.

The average photon number M_{\pm} over \mathbf{k}_1 with polarization $\vec{\pi}_{\pm}$ is found to depend on the phase φ as follows: $M_{\pm}(\varphi) = \bar{m} + \frac{1}{2}(2\bar{m} + 1)(1 \pm \cos \varphi)$ with $\bar{m} = \sinh^2 g$. The average photon number related to both cases is: $M_+(0) = 3\bar{m} + 1$ and $M_+(\pi) = \bar{m}$. The average number of photons emitted over the two polarizations over \mathbf{k}_1 is found to be $M = 4\bar{m} + 1$. The sinusoidal fringe pattern of the field intensity has now visibility $\mathcal{V}_{PC}^{th} = \frac{2\bar{m}+1}{4\bar{m}+1}$ (De Martini, 1998b). Note that for $g \rightarrow \infty$, the fringe visibility attains the asymptotic values $\mathcal{V}_{PC}^{th} = (\frac{1}{2})$.

III. OPTIMAL QUANTUM MACHINES VIA PARAMETRIC AMPLIFICATION

In the early eighties (Dieks, 1982; Ghirardi, 1981; Wootters and Zurek, 1982) demonstrated the impossibility of perfectly copying an unknown arbitrary quantum state. In other words, a "universal machine" mapping $|\Psi\rangle \rightarrow |\Psi\rangle|\Psi\rangle$ for every $|\Psi\rangle$ cannot be physically realized. More generally, an exact, universal cloner of N qubits into $M > N$ qubits cannot exist. Of course perfect cloning can be provided by a "non-universal" cloning machine, i.e. one made for one or a restricted class of states. Let us consider the following scenario: in order to copy the quantum state of qubit C , we couple it with another "ancilla" T in the state $|0\rangle$ by adopting a two qubit logical gate: a Control-NOT (C-NOT). By this approach it is possible to perfectly copy the state $|0\rangle_C$ or $|1\rangle_C$ using the qubit to be copied as control qubit and an ancilla qubit in the state $|0\rangle_T$ as target one (Nielsen and Chuang, 2000). However, starting from any general state $|\phi\rangle_C = \alpha|0\rangle_C + \beta|1\rangle_C$ the output state generated by the C-NOT gate is $\alpha|0\rangle_C|0\rangle_T + \beta|1\rangle_C|1\rangle_T$ with $\rho_C = \rho_T = |\alpha|^2|0\rangle\langle 0| + |\beta|^2|1\rangle\langle 1|$, which are clearly different from the initial state $|\phi\rangle\langle\phi|$. Hence the quantum C-NOT realizes a perfect cloning machine only for the two input qubit belonging to the set $\{|0\rangle, |1\rangle\}$. Of course these limitations are effective within the quantum world, i.e. whenever the quantum superposition character of the state dynamics is a necessary property of the system, as in an interferometer or, more generally in a quantum computer.

The no-cloning theorem has also interesting connections with the impossibility of superluminal communication (generally called "no-signaling condition") (Simon *et al.*, 2001). That condition will be discussed in details in Section IV.

We shall see that an approximate, "optimal" solution for cloning, as well for other quantum processes which are impossible in their "exact" form, is possible however. By definition, the "optimal" solutions correspond to the best maps realizable by Nature, i.e., the ones that work just on the boundaries corresponding to the limitations imposed by the principles of quantum mechanics.

The concept of optimal cloning process has been first

worked out in a seminal paper by (Buzek and Hillery, 1996). A transformation which produces two copies ($M = 2$) in the same mixed state ρ_{Cl} out of an arbitrary input qubit $|\phi\rangle$ ($N = 1$) was introduced with a fidelity equal to

$$\mathcal{F}_{1 \rightarrow 2}(|\phi\rangle, \rho_{Cl}) = \langle\phi|\rho_{Cl}|\phi\rangle = \frac{5}{6} \quad (11)$$

This map was demonstrated to be optimal in the sense that it maximizes the average fidelity between the input state and output qubits in (Bruß *et al.*, 1998; Bruss *et al.*, 1998; Werner, 1998; ?). More generally, in (?) a quantum cloning machine has been investigated which transforms N identical qubits into M identical copies with an optimal fidelity. In summary, the universal quantum cloning machine, which transforms N identical qubits $|\phi\rangle$ into M identical copies ρ_{Cl} , achieves as optimal fidelity:

$$\mathcal{F}_{N \rightarrow M}(|\phi\rangle, \rho_{Cl}) = \frac{N + 1 + \beta}{N + 2} \quad (12)$$

with $\beta \equiv N/M \leq 1$ (Bruss *et al.*, 1998; Buzek and Hillery, 1998; ?). It is useful to compare the previous approach with the process of "state estimation". Suppose to have N copies of the same quantum state $|\varphi\rangle$ and to wish to determine all the parameters which characterize $|\varphi\rangle$. The optimal estimation procedure leads to a fidelity between the input state and the estimated one equal to $\mathcal{F}_{est} = \frac{N+1}{N+2}$. As we can see $\mathcal{F}_{N \rightarrow M}(|\phi\rangle, \rho_{Cl})$ is larger than the one obtained by the N estimation approach and reduces to that result for $\beta \rightarrow 0$, i.e. for an infinite number of copies: $M \rightarrow \infty$. The extra positive term β in the above expression accounts for the excess of quantum information which, originally stored in N states, is optimally redistributed by entanglement among the $M - N$ remaining blank ancilla qubits (Buzek and Hillery, 1996).

In addition to the above results, less "universal" cloning machines have been investigated (Bruss *et al.*, 1998; Buzek *et al.*, 1997), where the state-dependent cloner is optimal with respect to a given ensemble of states. As discussed later, this process, generally referred to as "covariant cloning", operates with a higher fidelity than for the universal cloning since there is a partial a-priori knowledge of the state (11).

The study of optimal quantum cloning is interesting since it implies an insightful understanding of the critical boundaries existing between classical and quantum information processing. In the quantum information perspective, the optimal cloning process may be viewed as providing a distribution of quantum information over a larger system in the most efficient way (Ricci *et al.*, 2005). More details on the general cloning process can be found in the reviews (Scarani *et al.*, 2005), (De Martini and Sciarrino, 2005) and (Cerf and Fiurasek, 2006).

A. Universal optimal quantum cloning

Since the first articles on no-cloning theorem it was proposed to exploit the QED stimulated emission process in order to make imperfect copies of the polarization state of single photons (Mandel, 1983; Milonni and Hardies, 1982). (De Martini, 1998a; De Martini *et al.*, 2000; Simon *et al.*, 2000) showed that the optimal universal quantum cloning can indeed be realized by this method. If polarization encoding is adopted, the "universality" of this scheme is achieved by choosing systems that have appropriate symmetries, i.e., having a stimulated emission gain g which is polarization independent. This condition can be achieved by adopting a laser medium or a QI-OPA amplifier working in the non-collinear configuration. The present Section deals explicitly with this scheme.

As first scenario we will consider the $1 \rightarrow 2$ universal cloning. Precisely the action of the cloner can be described by the following covariant transformation (Buzek and Hillery, 1996):

$$|\Psi\rangle_{C1} |0\rangle_{C2} |0\rangle_{AC} \implies \sqrt{2/3} |\Psi\rangle_{C1} |\Psi\rangle_{C2} |\Psi^\perp\rangle_{AC} - \sqrt{1/3} |\{\Psi, \Psi^\perp\}\rangle_{C1,C2} |\Psi\rangle_{AC} \quad (13)$$

where the first state vector, in the left-hand side of equation (13), corresponds to the system to be cloned, the second state vector describes the system on which the information is to be copied ("blank" qubit), represented by the "cloning channel" (C), the mode \mathbf{k}_1 , while the third state vector represents the cloner machine. The blank qubit and the cloner are initially in the known state $|0\rangle$. The state $|\{\Psi, \Psi^\perp\}\rangle$ is the symmetrized state of the two qubit: $2^{-\frac{1}{2}}(|\Psi\rangle|\Psi^\perp\rangle + |\Psi^\perp\rangle|\Psi\rangle)$.

At the outputs of the cloner $C1$ and $C2$, we find two qubits, the original and the copy, each one with the following density matrix:

$$\rho_{C1} = \rho_{C2} = \frac{5}{6} |\Psi\rangle\langle\Psi| + \frac{1}{6} |\Psi^\perp\rangle\langle\Psi^\perp| \quad (14)$$

The density operators ρ_{C1} and ρ_{C2} describe the best possible approximation of the perfect universal cloning process. The fidelity of this transformation does not depend on the state of the input and is equal to (11). The cloner itself after the cloning transformation is in the state $\rho_{AC} = 1/3 |\Psi^\perp\rangle\langle\Psi^\perp| + 1/3 \times \mathbf{I}$, where \mathbf{I} is the unity operator and is related to the Universal NOT gate, as we shall see later.

Let's now establish a close connection of the above cloning results with the non-collinear QI-OPA system. The photon injected in the mode \mathbf{k}_1 has a generic polarization state corresponding to the unknown input qubit $|\Psi\rangle$. We shall describe this polarization state as $\hat{a}_\Psi^\dagger |0, 0\rangle_1 = |1, 0\rangle_1$ where $|m, n\rangle_1$ represents a state with m photons having the polarization Ψ , and n photons with polarization Ψ^\perp on the mode \mathbf{k}_1 . Let's assume that the mode \mathbf{k}_2 is initially in the vacuum state. The initial polarization state is hence expressed as $|\Psi\rangle_{in} =$

$|1, 0\rangle_1 \otimes |0, 0\rangle_2$ and evolves according to the unitary operator $\hat{U}_U \equiv \exp(-i\hat{H}_U t/\hbar)$ (see Section II-A):

$$\hat{U}_U |\Psi\rangle_{in} \simeq |1, 0\rangle_1 \otimes |0, 0\rangle_2 + g \left(\sqrt{2} |2, 0\rangle_1 \otimes |0, 1\rangle_2 - |1, 1\rangle_1 \otimes |1, 0\rangle_2 \right) \quad (15)$$

The linearization procedure implying the above approximation is justified in the present scenario by the small value of the amplification gain: $g \approx 0.1$ (De Martini *et al.*, 2002, 2004). The zero order term in Eq.(15) corresponds to the process when the input photon in the mode \mathbf{k}_1 did not interact in the non-linear medium, while the second term describes the first order amplification process. Here the state $|2, 0\rangle_1$ describing two photons of the mode \mathbf{k}_1 in the polarization state Ψ corresponds to the state $|\Psi\Psi\rangle$.

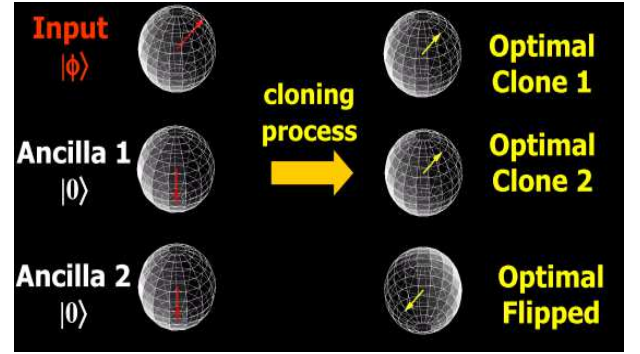


FIG. 2 Scheme of the optimal cloning process. The input and output qubit are represented on the Bloch sphere. The vectors associated to the output states are shrunk compared to the input state $|\phi\rangle$.

To see that the stimulated emission is indeed responsible for creation of the cloned qubit, let us compare the state Eq. (15) with the output of the optical parametric amplifier when the vacuum is injected into the crystal on both input modes \mathbf{k}_i ($i = 1, 2$). In this SPDC case the input state is $|0\rangle_{in} = |0, 0\rangle_1 \otimes |0, 0\rangle_2$, and we obtain to the same order of approximation as above:

$$\hat{U}_U |0\rangle_{in} \simeq |0, 0\rangle_1 \otimes |0, 0\rangle_2 + g \left(|1, 0\rangle_1 \otimes |0, 1\rangle_2 - |0, 1\rangle_1 \otimes |1, 0\rangle_2 \right) \quad (16)$$

We see that the cloned qubits, described by the state vector $|1, 0\rangle_1$ in the right-hand sides of equations (15) and (16), do appear with different amplitudes, corresponding to the ratio of the probabilities: $R = 2$. It is easy to show that the fidelity of the output clone is found to be $\frac{2R+1}{2R+2} = \frac{5}{6}$ and is optimal.

A more general analysis can be undertaken by extending the isomorphism discussed above to a larger number of input and output particles N and M . In this case it is found that the QI-OPA amplification process \hat{U}_U in each order of the decomposition into the parameter g corresponds to the $N \rightarrow M$ cloning process. Precisely,

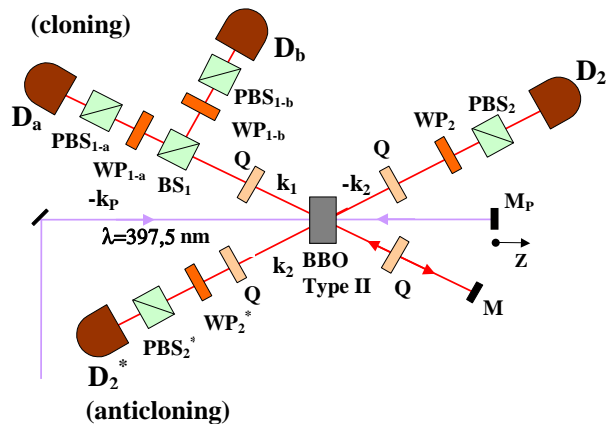


FIG. 3 Schematic diagram of the *universal optimal cloning machine* realized on the cloning (C) channel (mode \mathbf{k}_1) of a *self-injected* OPA and of the Universal NOT gate realized on the anticloning (AC) channel, \mathbf{k}_2 (De Martini *et al.*, 2004).

in this case $M \geq N$ output particles are detected over the output cloning mode, \mathbf{k}_1 . Correspondingly, $M - N$ particles are detected over the output anticloning mode, \mathbf{k}_2 . The cloning transformation is realized *a posteriori* in the sense that the output number M of copies is a random variable that is selected as the result of the measurement of the photon number in the anticloning beam (Simon *et al.*, 2000).

It appears clear, from the above analysis, that the effect of the input vacuum field which is necessarily injected in any universal optical amplifier, is indeed responsible to reduce the fidelity of the quantum cloning machines at hand. More generally, the vacuum field is in precise correspondence with, and must be interpreted as, the amount of QED vacuum fluctuations that determines the upper bounds to the fidelity determined by the structure of quantum mechanics.

The universal cloning has been realized by exploiting the stimulated emission induced by a single photon by (De Martini *et al.*, 2002, 2004; Pelliccia *et al.*, 2003) as shown in Figure 3. There a spontaneous parametric down conversion process excited by the $-\mathbf{k}_p$ pump mode created single pairs of photons with equal wavelengths in entangled singlet states of linear polarization. One photon of each pair, emitted over $-\mathbf{k}_1$, was reflected by a spherical mirror into the crystal where it provided the $N = 1$ single photon injection into the optical parametric amplifier excited by the pump beam associated with the backreflected mode \mathbf{k}_p . Hence the optimal cloning process was realized along the mode \mathbf{k}_1 . A similar experiment has been reported by (Lamas-Linares *et al.*, 2002) where the single photon initial qubit was implemented by a highly attenuated coherent state beam.

B. Universal optimal NOT gate

The "NOT gate", the transformation that maps any qubit onto the orthogonal qubit, i.e. onto its antipode on the Bloch sphere, has been recognized to be impossible according to the principles of quantum mechanics (Bechmann-Pasquinucci and Gisin, 1999). In fact if $|\Psi\rangle = \alpha|0\rangle + \beta|1\rangle$ is a generic qubit, its antipode is generated by the "time reversal" transformation $T|\Psi\rangle = |\Psi^\perp\rangle = \beta^*|0\rangle - \alpha^*|1\rangle$ such that $\langle\Psi|\Psi^\perp\rangle = 0$. As it is well known T , being an anti-unitary transformation is not allowed by quantum mechanics: it may be expressed as: $T = \sigma_y K$ being K the transposition or "phase conjugation" map (Nielsen and Chuang, 2000). All this is at variance with the notion of classical information theory by which the NOT gate is the simplest operation to be performed "exactly" on any classical bit. The optimal approximation of the Universal NOT gate (U-NOT) maps N identical input qubits $|\phi\rangle$ into M optimally flipped ones in the state σ_{out} and achieves the fidelity :

$$\mathcal{F}_{N \rightarrow M}^*(|\phi^\perp\rangle, \sigma_{out}) = \langle\phi^\perp|\sigma_{out}|\phi^\perp\rangle = \frac{N+1}{N+2} \quad (17)$$

We note that $\mathcal{F}_{N \rightarrow M}^*$ depends only on the number of the input qubits (Buzek *et al.*, 1999; Gisin and Popescu, 1999; Bužek and Hillery, 2000). Indeed the fidelity of the U-NOT gate is exactly the same as the optimal quantum estimation fidelity (Massar and Popescu, 2009). This means that the realization of this process is equivalent to a classical preparation of M identical flipped qubits following an approximate quantum estimation of N input states. Only this last operation is affected by noise and in the limit $N \rightarrow \infty$ a perfect estimation of the input state is achieved leading to the realization of an exact flipping operation.

Let's consider again the expression (15) of the output state of the optical parametric amplifier. The vector $|0, 1\rangle_2$ describes the state of the mode \mathbf{k}_2 with a single photon in the polarization state $|\Psi^\perp\rangle$. This state vector represents the flipped version of the input qubit on mode \mathbf{k}_1 and then the QI-OPA acts on the output mode \mathbf{k}_2 as a Universal NOT-gate (De Martini *et al.*, 2002). We see that the flipped qubit described by the state vector $|0, 1\rangle_2$ in the right-hand sides of Eqs.(15) and (16) do appear with different amplitudes corresponding to the ratio of probabilities: $R^* = 2 : 1$. Note in Eqs.(15), (16) that, by calling by R the ratio of the probabilities of detecting 2 and 1 photons on mode \mathbf{k}_1 only, we obtain: $R = R^*$. In other words, the *same value* of signal to noise ratio affects both cloning and U-NOT processes realized simultaneously on the two different output modes: \mathbf{k}_1 and \mathbf{k}_2 . The corresponding values of the U-NOT fidelity reads $\mathcal{F}^* = 2/3$ and is equal to the optimal one allowed by quantum mechanics (De Martini *et al.*, 2002).

A remarkable and somewhat intriguing aspect of the present process is that both processes of quantum cloning and the U-NOT gate are realized contextually by the *same* physical apparatus, by the same unitary transfor-

mation and correspondingly by the same quantum logic network (De Martini *et al.*, 2004).

The relation between the cloning and the NOT operations have been latter discussed according to the conservation laws alone (van Enk, 2005). It was suggested that the close link existing between the limitations on cloning and NOT operations could express an as yet unexplored natural law. The result discussed above are general and hold both in classical and quantum-mechanical worlds, for both optimal and suboptimal operations, and for bosons as well as fermions.

C. Optimal machines by symmetrization

Optimal quantum cloning machines, although working probabilistically, have been demonstrated experimentally by a symmetrization technique (Irvine *et al.*, 2004; Ricci *et al.*, 2004; Sciarrino *et al.*, 2004a,b). This approach to the probabilistic implementation of the N to M cloning process has been first proposed by Werner (Werner, 1998). It is based on the action of a projective operation on the symmetric subspace of the N input qubits and $M - N$ blank ancillas. This transformation assures the uniform distribution of the initial information into the overall system and guarantees that all output qubits are indistinguishable. To achieve the projection over the symmetric subspace we exploit the bosonic nature of photons, viz. the exchange symmetry of their overall wavefunction. In particular we use a two-photon Hong-Ou-Mandel coalescence effect (Hong *et al.*, 1987). In this process, two photons impinging simultaneously on a beamsplitter from two different input modes have an enhanced probability of emerging along the same output mode (that is, "coalescing"), as long as they are indistinguishable. If the two photons are made distinguishable, e.g by different encoding of their polarization or of any other degree of freedom, the coalescence effect vanishes. Now, if one of the two photons involved in the process is in a known input state to be cloned and the other is in a random one, the coalescence effect will enhance the probability that the two photons emerge from the beamsplitter with the same quantum state. In other words, the symmetrization enhances the probability of a successful cloning detected at the output of the beamsplitter.

The universal optimal quantum cloning based on the symmetrization technique was first demonstrated for polarization encoded qubit (Irvine *et al.*, 2004; Ricci *et al.*, 2004; Sciarrino *et al.*, 2004a,b) and latter reported for orbital angular momentum-encoded qubits (Nagali *et al.*, 2009). Finally (Nagali *et al.*, 2010) reported the experimental realization of the optimal quantum cloning of four-dimensional quantum states, or ququarts, encoded in the (polarization + orbital angular momentum) degrees of freedom of photons (Marrucci *et al.*, 2011).

D. Phase-covariant optimal quantum cloning

In addition to the impossibility of universally cloning unknown qubits, there exists the impossibility of cloning subsets of qubits containing non orthogonal states. This no-go theorem has been adopted to provide the security of cryptographic protocols as *BB84* (Gisin *et al.*, 2002). Recently state dependent, non universal, optimal cloning machines have been investigated where the cloner is optimal with respect to a given ensemble (Bruß *et al.*, 2000). This partial a-priori knowledge of the state allows to reach a larger fidelity than for the universal cloning.

The simplest and most relevant case is represented by the cloning covariant under the Abelian group $U(1)$ of phase rotations, the so called "phase-covariant cloning". There, the information is encoded in the phase ϕ_i of the input qubit belonging to the equatorial plane i of the corresponding Bloch sphere. In this context the general state to be cloned may be expressed as: $|\phi_i\rangle = (|\psi_i\rangle + e^{i\phi_i} |\psi_i^\perp\rangle)$ and $\{|\psi_i\rangle, |\psi_i^\perp\rangle\}$ is a convenient orthonormal basis (Bruß *et al.*, 2000). The values of the optimal fidelities $\mathcal{F}_{cov}^{N \rightarrow M}$ for the phase-covariant cloning machine have been found in (D'Ariano and Macchiavello, 2003). Restricting the analysis to a single input qubit to be cloned $N = 1$ into $M > 1$ copies, the cloning fidelity is found: $\mathcal{F}_{cov}^{1 \rightarrow M} = \frac{1}{2} \left(1 + \frac{M+1}{2M}\right)$ for M assuming odd values, or $\mathcal{F}_{cov}^{1 \rightarrow M} = \frac{1}{2} \left(1 + \frac{\sqrt{M(M+2)}}{2M}\right)$ for M even. In particular we have $\mathcal{F}_{cov}^{1 \rightarrow 2} = 0.854$ and $\mathcal{F}_{cov}^{1 \rightarrow 3} = 0.833$ to be compared with the corresponding figures valid for universal cloning: $\mathcal{F}_{univ}^{1 \rightarrow 2} = 0.833$ and $\mathcal{F}_{univ}^{1 \rightarrow 3} = 0.778$. It is worth to enlighten the deep connection linking the phase-covariant cloning and the estimation of an equatorial qubit, that is, with the problem to finding the optimal strategy to estimate the value of the phase ϕ (Derka *et al.*, 1998). In general for $M \rightarrow \infty$, $\mathcal{F}_{cov}^{N \rightarrow M} \rightarrow \mathcal{F}_{phase}^N$. In particular we have $\mathcal{F}_{cov}^{1 \rightarrow M} = \mathcal{F}_{phase}^1 + \frac{1}{4M}$ with $\mathcal{F}_{phase}^1 = 3/4$.

We shall briefly review different schemes which can be realized through the methods of quantum optics outlined above (Sciarrino and De Martini, 2007). Let us restrict our attention to the $1 \rightarrow 3$ phase-covariant quantum cloning machine as the corresponding scheme can be easily extended to general case $1 \rightarrow M$ for odd values of M . The phase-covariant cloner can be realized by adopting a quantum-injected optical parametric amplifier (QI-OPA) working in a collinear configuration: Figure 1 c) (De Martini, 1998b). In this case the interaction Hamiltonian $\hat{\mathcal{H}}_{PC} = i\chi\hbar \left(\hat{a}_H^\dagger \hat{a}_V^\dagger\right) + h.c.$ acts on a single output spatial mode \mathbf{k} . A fundamental physical property of $\hat{\mathcal{H}}_{PC}$ consists of its rotational invariance under $U(1)$ transformations, that is, under any arbitrary rotation around the z -axis. Let us consider an injected single photon with polarization state $|\phi\rangle_{in} = 2^{-1/2}(|H\rangle + e^{i\phi}|V\rangle) = |1, 0\rangle_{\mathbf{k}}$ where $|m, n\rangle_{\mathbf{k}}$ represents a product state with m photons of the mode \mathbf{k} with polarization ϕ , and n photons with polarization ϕ^\perp . The first contribution to the amplified state, $\sqrt{6}|3, 0\rangle_{\mathbf{k}} - \sqrt{2}e^{i2\phi}|1, 2\rangle_{\mathbf{k}}$ is identical to

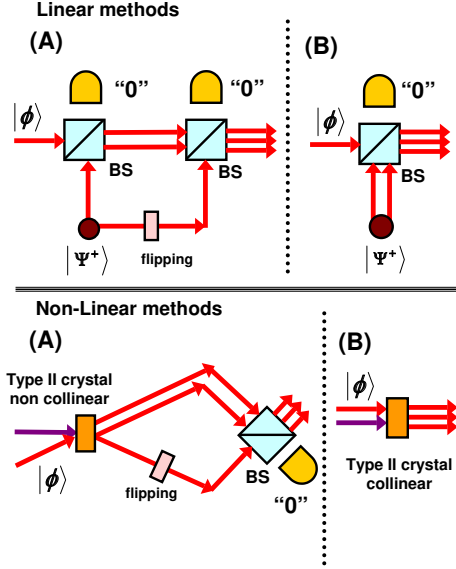


FIG. 4 Linear methods: (a) schematic diagram of the linear optics multi qubit symmetrization apparatus realized by a chain of interconnected Hong-Ou-Mandel interferometer; (b) symmetrization of the input photon and the ancilla polarization entangled pairs. Non-linear methods: (a) UQCM by optical parametric amplification, flipping by a couple of waveplates and projection over the symmetric subspace; (b) collinear optical parametric amplification (Sciarrino and De Martini, 2007).

the output state obtained from a $1 \rightarrow 3$ phase-covariant cloning. Indeed the fidelity is found to be the optimal one $F^{1 \rightarrow 3} = \frac{5}{6}$ (Sciarrino and De Martini, 2007). Notice the effect of the input vacuum field over the single \mathbf{k} mode with polarization ϕ^\perp coupled to the phase-covariant optical amplifier, this vacuum contribution is indeed responsible to reduce the fidelity of the quantum cloning machine.

Interestingly, the same overall state evolution can also be obtained at the output of a non-collinear QI-OPA together with a Pauli σ_Y operation and the projection of the three output photons over the symmetric subspace Fig.4(a). This scheme was experimentally realized by the following method: the flipping operation on the output mode \mathbf{k}_{AC} was realized by means of two waveplates, while the physical implementation of the symmetrization projector on the three photons-states was carried out by linearly superimposing the modes \mathbf{k}_C and \mathbf{k}_{AC} on a beam-splitter BS and then by selecting the case in which the three photons emerged from BS all on the same output mode \mathbf{k}_{PC} (Sciarrino and De Martini, 2005).

IV. PARAMETRIC AMPLIFICATION AND NO-SIGNALING THEOREM

In the present paragraph we review the connections between the cloning process and the special theory of relativity according to which any signal carrying information cannot travel at a speed larger than the velocity of light in vacuum: c . Even if quantum physics has marked nonlocal features due to the existence of entanglement, it has been found that a "no-signaling theorem" exists according to which one cannot exploit quantum entanglement between two space-like separated parties for "faster-than-light" communication (Maudlin, 2002). Several attempts to break this "peaceful coexistence" have been proposed, the most renowned one by Nick Herbert in 1981 by its FLASH machine (First Laser-Amplified Superluminal Hookup) (Herbert, 1982). The publication of this proposal, based on a cloner machine applied to an entangled state of two spacelike distant particles A and B , was followed by a lively debate that eventually stimulated the formulation of the "no-cloning theorem" (Wootters and Zurek, 1982).

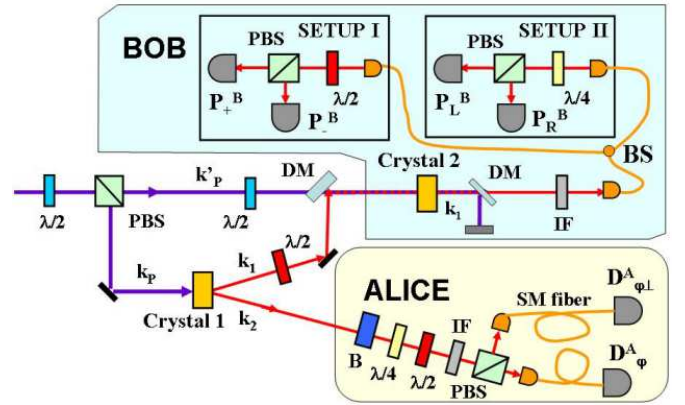


FIG. 5 Configuration of the quantum injected optical parametric amplifier. The SPDC quantum injector (crystal 1) is provided by a type II generator of polarization entangled photon couples (De Angelis *et al.*, 2007).

The setup proposed by Herbert is reported in Fig.5. If one observer, *Bob* by measuring the particle B could distinguish between different state mixtures that have been prepared by the distant observer *Alice* by measuring the particle A , then quantum non-locality could be used for signaling. Precisely, let's consider the following: Alice and Bob share two polarization entangled photons A and B generated by a common source. Alice detects her photon polarization with the detectors D_φ^A and $D_{\varphi^\perp}^A$ either in the basis $\{\vec{\pi}_\pm = 2^{-1/2}(\vec{\pi}_V \pm \vec{\pi}_H)\}$ or $\{\vec{\pi}_R = 2^{-1/2}(\vec{\pi}_H + i\vec{\pi}_V), \vec{\pi}_L = 2^{-1/2}(\vec{\pi}_V - i\vec{\pi}_H)\}$, where $\vec{\pi}_H$ and $\vec{\pi}_V$ are, respectively, linear horizontal and vertical polarization. If Bob could guess with a probability larger than $\frac{1}{2}$ the basis chosen by Alice, superluminal signaling would be established. It was recognized that this is impossible if the experiment involves two sin-

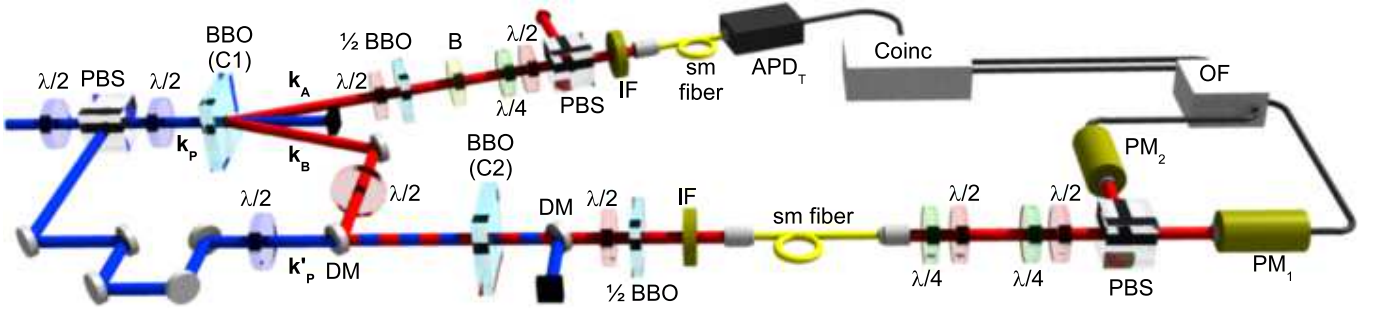


FIG. 6 Scheme of the experimental setup. The main ultraviolet laser beam provides the excitation field beam at $\lambda_P = 397.5\text{nm}$. A type II Beta Barium Borate crystal (crystal 1: C1) generates pair of photons with $\lambda = 795\text{nm}$. The photon belonging to \mathbf{k}_B , together with the pump laser beam \mathbf{k}'_p , is fed into an high gain optical parametric amplifier consisting of a crystal 2 (C2), cut for collinear type-II phase matching. Measurement apparatus: the field is analyzed by two photomultipliers (PM₁ and PM₂) and then discriminated through an O-Filter device (OF), whose action is described in the text. For more details refer to (De Martini *et al.*, 2008).

gle particles. However Herbert thought that Bob could make a "new kind" of measurement involving the amplification of the received signal B through a "nonselective laser gain tube", viz, a universal (polarization independent) amplifier. The amplified photon beam is "split" by an optical "beam splitter" (BS), so Bob can perform on one of the two output channels of BS a measurement on half of the cloned particles by an apparatus tuned on the basis $\{\vec{\pi}_\pm\}$ who records the signal I_\pm^B . Simultaneously, he could record on the other BS output channel the signals $I_{R/L}^B$ by an apparatus tuned on the basis $\{\vec{\pi}_R, \vec{\pi}_L\}$. In that way he could guess the right preparation basis carried out by Alice on particle A.

In order to test the Herbert's scheme a careful theoretical and experimental analysis of the output field was carried out with emphasis on fluctuations and correlations (De Angelis *et al.*, 2007). Precisely, the Herbert's scheme was reproduced by the optical parametric amplification of a single photon of an entangled pair into an output field involving 5×10^3 photons. Fig.5. Unexpected and pe-

culiar field correlations amongst the cloned particles preventing any violation of the no-signaling conditions have been found. Precisely, it was found that the limitations implied by a complete quantum cloning theory are not restricted to the bounds on the cloning fidelity but also largely affect the high-order correlations existing among the different clones. In fact, in spite of a reduced fidelity, noisy but separable, i.e., noncorrelated, copies would lead to a perfect state estimation for $g \rightarrow \infty$ and hence to a real possibility of superluminal communication. However, surprisingly enough the particles produced by any optimal cloning machine are highly interconnected and the high-order correlations are actually responsible for preventing any possibility of faster than light communication (Bae and Acín, 2006; De Angelis *et al.*, 2007; Demkowicz-Dobrzanski, 2005). Recently (Zhang *et al.*, 2011) investigated the wavepacket propagation of a single photon and showed experimentally in a conclusive way that the single photon speed is limited by c .

V. EXPERIMENTAL MACROSCOPIC QUANTUM SUPERPOSITION BY MULTIPLE CLONING OF SINGLE PHOTON STATES

A. Generation and detection of multi-particle quantum superpositions

The present Section accounts for the optical parametric amplification of a single photon in the high gain regime to experimentally investigate how the information initially contained in its polarization state is distributed over a large number of particles. In particular we analyze how the coherence properties of the input state are transferred to the mesoscopic output field.

Let's consider the scenario in which a single-particle qubit $|\psi\rangle_B = \alpha|\phi\rangle_B + \beta|\phi^\perp\rangle_B$, with $|\alpha|^2 + |\beta|^2 = 1$,

injected in a three-wave optical parametric amplifier (Yariv, 1989) is transformed by the unitary QI-OPA operation into a corresponding macroscopic quantum superposition (MQS):

$$|\Phi\rangle_B = \alpha|\Phi^\phi\rangle_B + \beta|\Phi^{\phi^\perp}\rangle_B \quad (18)$$

The multi-particle states, or macrostates, whose detailed expression reported in Eq.10, bear peculiar properties that deserve some comments. The macrostates, $|\Phi^\phi\rangle_B$, $|\Phi^{\phi^\perp}\rangle_B$ are orthonormal and exhibit observables bearing macroscopically distinct average values. Precisely, the average number of photons associated with the polarization mode $\vec{\pi}_\phi$ is: $\bar{m} = \sinh^2 g$ for $|\Phi^{\phi^\perp}\rangle_B$, and $(3\bar{m} + 1)$ for $|\Phi^\phi\rangle_B$. For the π -mode $\vec{\pi}_{\phi^\perp}$, orthogonal to $\vec{\pi}_\phi$, these values are interchanged among the two states. On

the other hand, as shown by (De Martini, 1998a), by changing the representation basis from $\{\vec{\pi}_\phi, \vec{\pi}_{\phi^\perp}\}$ to $\{\vec{\pi}_H, \vec{\pi}_V\}$, the same macro-states, $|\Phi^\phi\rangle_B$ or $|\Phi^{\phi^\perp}\rangle_B$ are found to be again quantum superpositions of two orthonormal states $|\Phi^H\rangle_B, |\Phi^V\rangle_B$, but differing by a single quantum. This unexpected and quite peculiar combination, i.e. a large difference of a measured observable when the states are expressed in one basis and a small Hilbert-Schmidt distance of the same states when expressed in another basis turned out to be a fundamental property that renders the coherence properties of the system robust toward the coupling with environment. This will be discussed later in Section VII. .

Let us first briefly review the adopted optical system adopted making reference to the experimental layout shown by the sketchy Figure 1 (c), or by the equivalent, more detailed Figure 6(Caminati *et al.*, 2006c; De Martini *et al.*, 2008; Nagali *et al.*, 2007). An entangled pair of two photons in the singlet state $|\psi^-\rangle_{A,B}=2^{-\frac{1}{2}}(|H\rangle_A|V\rangle_B - |V\rangle_A|H\rangle_B)$, was produced through spontaneous parametric down-conversion (SPDC) by the BBO crystal 1 (C1) pumped by a (weak) pulsed ultraviolet pump beam: Fig.6. There the labels A, B refer to particles associated respectively with the two output spatial modes \mathbf{k}_A and \mathbf{k}_B of the SPDC generated by C1. In the experiment the three spatial modes involved in the injected parametric interaction were carefully selected adopting single mode fibers. Consequently, in virtue of Equations (1, 2) a three-wave, collinear "phase-matching" condition was realized leading to a lossless amplification process.

The single photon qubit on mode \mathbf{k}_A of Fig. 6 (i.e. \mathbf{k}_2 in Fig. 1(c)) was sent to a "polarizing beam splitter" (PBS) whose output modes were coupled to two single-photon detectors. In a first experiment, these two detectors were simply connected as to merely identify the emission of A (and of B) without any effective polarization measurement on A . In other words, the two detectors acted as the single detector unit D_2 of the simplified Figure 1 c) by supplying a single electronic "trigger signal" for the overall experiment in correspondence with the emission of any entangled couple A, B emitted by C1. In virtue of this "trigger signal" the overall measurement of the MQS $|\Phi\rangle_B$ could be considered "heralded by", i.e. measured in coincidence with any photon A measured on mode \mathbf{k}_A . Accordingly, no bipartite Micro-Macro entanglement was detectable(De Martini, 1998b; De Martini *et al.*, 2008).

The single particle qubit $|\psi\rangle_B = 2^{-\frac{1}{2}}(|H\rangle_B - |V\rangle_B)$ associated with particle B , prepared in the superposition state of polarization state was then injected, together with a very intense laser pulsed pump beam, into the main optical parametric amplifier consisting of a second BBO crystal 2 (C2). The crystal C2 was oriented for "collinear operation", i.e., emitting pairs of amplified photons over the same output spatial mode supporting two orthogonal polarization modes, respectively horizon-

tal and vertical. The high - gain parametric amplification provided by the crystal C2 transformed the single - particle qubit: $|\psi\rangle_B$ into the corresponding multiparticle MQS: $|\Phi\rangle_B = 2^{-\frac{1}{2}}(|\Phi^\phi\rangle_B - |\Phi^{\phi^\perp}\rangle_B)$. This MQS, composed of $M \approx 5 \times 10^4$ photons, was analyzed by a "polarization analyzer" $[A(\varphi)]$ coupled through a PBS to two high-gain photomultipliers (PM) with detection efficiency $\simeq 5\%$. The device $A(\varphi)$ composed by a optical rotator and of a birefringent plate analyzed the MQS $|\Phi\rangle_B$ in a rotating base characterized by a single φ -phase. More details are given in:(De Martini, 1998b).

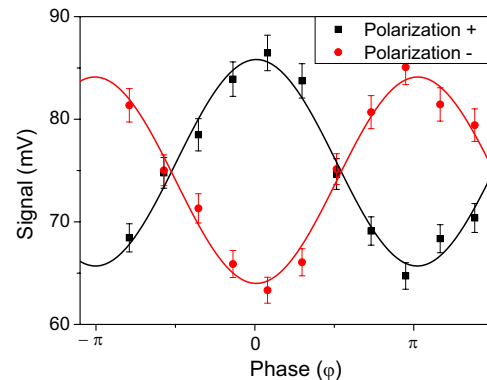


FIG. 7 Average signal versus the phase of the input qubit (Nagali *et al.*, 2007).

The sinusoidal behaviour shown by the detected experimental interference-fringe pattern reported in Fig.9 as function of φ , offers a visual realization of the original 1935 pictorial argument by Erwin Schrödinger (Schrödinger, 1935). These interference-fringe patterns show how the coherent quantum superposition properties of the input state can be transferred to the mesoscopic output, involving up a very large number of photon particles. There the minima and the maxima of the patterns, e.g. shown by Fig.7, could be attributed to the dead/alive conditions of the celebrated Schrödinger feline, i.e of the Macro-system. Similar MQS interference fringe - patterns arising in different experiments have been obtained: e.g. as shown by Figure 9, below and by Figure 4 of (De Angelis *et al.*, 2007). As already mentioned, all MQS results were obtained at "room temperature" thus defying the "phase-disrupting" decoherence process that generally affects this kind of experiment. However we shall see that the observation of other sophisticated quantum effects such as the entanglement correlations within Micro-Macro systems requires not only a system well protected against environmental decoherence, but also a sufficient measurement resolution. We shall see also that, in spite of the reported successful evidence of the MQS realization, the measurement of bipartite Micro-Macro entanglement with very large M meets severe experimental problems, owing to a newly discovered multiparticle "efficiency loophole"(Sekatski *et al.*, 2009). However, by a different quantum tomographic test within a "deliberate attenuation" experiment carried out in a non-collinear

configuration, the achievement of bipartite Micro-Macro entanglement was demonstrated for a limited number of QI-OPA generated particles: $M \leq 12$ (De Martini *et al.*, 2005) The last experiment, demonstrating the achievement of bipartite Micro-Macro entanglement as well as of the MQS condition, will be discussed below, in Sections VI and IX.



FIG. 8 Picture of the experimental apparatus adopted for the amplification of entangled pairs of photons (Quantum Optics Group, Dipartimento di Fisica, Sapienza Università di Roma).

VI. MICRO-MACRO SYSTEM: HOW TO DEMONSTRATE ENTANGLEMENT

Owing to the close similarity existing between the QI-OPA scheme shown in Figure 1-c) and the well known EPR scheme it may be argued that the non-local separability between the single photon qubit $|\psi^-\rangle_{A,B} = 2^{-\frac{1}{2}}(|H\rangle_A|V\rangle_B - |V\rangle_A|H\rangle_B)$ emitted over the output mode \mathbf{k}_B and the Macro-state emitted over \mathbf{k}_A could be demonstrated experimentally (Caminati *et al.*, 2006c). Formally, this endeavor would consist of the demonstration of the existence of the entangled state connecting the two Micro-Macro systems A and B :

$$|\Psi^-\rangle_{AB} = \frac{1}{\sqrt{2}}(|\phi\rangle_A|\Phi^{\phi_\perp}\rangle_B - |\phi_\perp\rangle_A|\Phi^\phi\rangle_B) \quad (19)$$

There the output macro state is expressed by $|\Phi^\phi\rangle = \hat{U}_{PC}|\phi\rangle$, where $|\phi\rangle$ labels the injection of single-photon state is (7).

Such a demonstration would consist of a complete physical achievement of the 1935 Schrödinger Cat program. In the following subsections different theoretical and experimental approaches will be briefly discussed. In particular, an ambitious attempt in this direction was

undertaken with a high gain QI-OPA method generating a Macro state consisting of nearly $M = 10^4$ photons. The experimental layout was similar to the one described in Section V but adopted a different, sophisticated processing of the signals generated by the particle detectors (De Martini *et al.*, 2008). However, it was soon realized that a conclusive test of Micro-Macro entanglement for a very large number of particles could only be achieved successfully by adoption of linear photomultipliers featuring a very large detection efficiency $\eta \lesssim 1$, a condition not made available by the present technology (Sekatski *et al.*, 2009). This is but the effect of a new form of the well known "detection loophole" which affects in general all nonlocality tests and is found to worsen for an increasing number M of detected particles. However, as said, in spite of all these problems a conclusive experimental demonstration of Micro-Macro entanglement has been realized by a quantum tomographic method for a limited number of MQS particles: $M \lesssim 12$, as we shall immediately see in the next paragraph.

1. Extracted two photon density matrices

A feasible approach for the analysis of multiphoton fields is based on the deliberate attenuation of the analyzed system up to the single photon level (Eisenberg *et al.*, 2004). In this way, standard single-photon techniques and criteria can be used to investigate the properties of the field. The verification of the bi-partite entanglement in the high loss regime is an evidence of the presence of entanglement before attenuation, on the premise that no entanglement can be generated by any "local operations", including lossy attenuation. The attenuation method has been applied to the Micro-Macro system, realizing by a quantum tomographic method the experimental proof of the presence of entanglement between the single photon state of mode \mathbf{k}_A and the multiphoton state with $M \lesssim 12$ of mode \mathbf{k}_B generated through the process of parametric amplification in an universal cloning configuration: Figure 6. The theory of this experiment will be considered once again, in more details in Section IX, below (Caminati *et al.*, 2006a; De Martini *et al.*, 2005). Unfortunately, such approach could only be applied for a very limited number M , since in practice unavoidable experimental imperfections quickly wash out any evidence of entanglement (Spagnolo *et al.*, 2010c).

2. Pseudo-spin operators

Let us now address a different criteria to verify the bipartite entanglement between the modes \mathbf{k}_A and \mathbf{k}_B . We adopt the standard Pauli operators for the single photon polarization state belonging to mode \mathbf{k}_A . We introduce a formalism useful to associate the amplified multi-particle field on mode \mathbf{k}_B to a Macro-qubit.

Through the amplification process the spin operators $\hat{\sigma}_i$ of the single photon evolve into the "macro-spin" operators $\hat{\Sigma}_i$ for the many particle system $\hat{\Sigma}_i = \hat{U}\hat{\sigma}_i\hat{U}^\dagger = |\Phi^{\psi_i}\rangle\langle\Phi^{\psi_i}| - |\Phi^{\psi_{i\perp}}\rangle\langle\Phi^{\psi_{i\perp}}|$. The operators $\{\hat{\Sigma}_i\}$ satisfy the same commutation rules of the single particle $\frac{1}{2}$ -spin $[\hat{\Sigma}_i, \hat{\Sigma}_j] = \varepsilon_{ijk} 2i\hat{\Sigma}_k$ where ε_{ijk} is the Levi-Civita tensor density. Hence the generic state $\alpha|\Phi^H\rangle_B + \beta|\Phi^V\rangle_B$ can be handled as a qubit in the Hilbert space H_B spanned by $\{|\Phi^H\rangle_B, |\Phi^V\rangle_B\}$. To test whether the output state is entangled, one should measure the correlation between the single photon spin operator $\hat{\sigma}_i^A$ on the mode \mathbf{k}_A and the macro-spin operator $\hat{\Sigma}_i^B$, on the mode \mathbf{k}_B . We then adopt the criteria for two qubit bipartite systems based on the spin-correlation. We define the visibility $V_i = \left| \langle \hat{\Sigma}_i^B \otimes \hat{\sigma}_i^A \rangle \right|$ a parameter which quantifies the correlation between the systems A and B . The value $V_i = 1$ corresponds to perfect anti-correlation, while $V_i = 0$ expresses the absence of correlation. The following upper bound criterion for a separable state holds (Eisenberg *et al.*, 2004): $S = \sum_i V_i \leq 1$. In order to measure the expectation value of $\hat{\Sigma}_i^B$, a discrimination among the pair of states $\{|\Phi^{\psi_i}\rangle, |\Phi^{\psi_{i\perp}}\rangle\}$ for the three different polarization bases 1, 2, 3 is required. Consider the two macro-states $|\Phi^+\rangle$ and $|\Phi^-\rangle$. A perfect discrimination can be achieved by identifying whether the number of photons over the \mathbf{k}_B mode with polarization $\vec{\pi}_+$ is even or odd. As already said, this requires the detection of the mesoscopic field by a photon-number-resolving detectors operating with an overall quantum efficiency $\eta \approx 1$, a device not yet made available by the present technology. We face here the problem of detecting correlations by performing a coarse-grained measurement process.

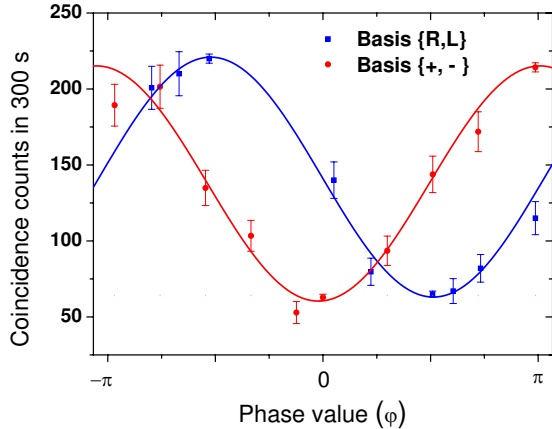


FIG. 9 Coincidence counts $[L_B; D_A]$ versus the phase of the injected qubit for the diagonal (circle data) and circular polarization basis (square data) (De Martini *et al.*, 2008).

3. Correlation measurements via orthogonality filter

In order to implement a measurement with high-discrimination, a new method has been adopted, viz. the O-Filter (OF) based strategy. This method is based on a probabilistic discrimination of the macro-states $|\Phi^\phi\rangle$ and $|\Phi^{\phi\perp}\rangle$, which exploits the macroscopic features present in their photon-number distributions (Nagali *et al.*, 2007). Such measurement is implemented by an intensity measurement carried out by multiphoton linear detectors in the $\{\vec{\pi}_i, \vec{\pi}_i^\perp\}$ basis, followed by an electronic processing of the recorded signal. If $n_\pi - m_{\pi\perp} > k$, the (+1) outcome is assigned to the event, if $m_{\pi\perp} - n_\pi > k$ the (-1) outcome is assigned to the event. If $|n_\pi - m_{\pi\perp}| < k$, an inconclusive outcome (0) is assigned to the event.

Experimentally the photon is detected on mode \mathbf{k}_A adopting single photon detectors and the multiphoton field of mode \mathbf{k}_B with photomultipliers and O-Filter. The experimental fringe patterns shown in Fig.9 were obtained by adopting the common analysis basis $\{\vec{\pi}_R, \vec{\pi}_L\}$ with a filtering probability $\simeq 10^{-4}$. In this case the average visibility has been found $V_2 = (54.0 \pm 0.7)\%$. A similar oscillation pattern has been obtained in the basis $\{\vec{\pi}_+, \vec{\pi}_-\}$ leading to: $V_3 = (55 \pm 1)\%$. Since always is $V_1 > 0$, the experimental result $S = V_2 + V_3 = (109.0 \pm 1.2)\%$ should imply the violation of the separability criteria introduced above. However a careful analysis of the implications of discarding part of the data via the OF measurement should be addressed.

The state after losses is no more a macro-qubit living in a two dimensional Hilbert space, but in general it is represented by a density matrix $\hat{\rho}_\eta^\phi$. A detailed discussion on the properties of the macrostates after losses in both the Fock-space and the phase-space is reported in (De Martini *et al.*, 2009a; Spagnolo *et al.*, 2009, 2010c). Very generally, the probabilistic detection method described above can be adopted to infer the active generation *before* losses of a Macro-state $|\Phi^\phi\rangle$, or $|\Phi^{\phi\perp}\rangle$, by exploiting the information encoded in the unbalancement of the number of particles present in the state *after* losses $\hat{\rho}_\eta^\phi$. Hence the adopted entanglement criterion allowed to infer the presence of bipartite Micro-Macro entanglement present before losses, under a specific assumption (De Martini *et al.*, 2008). This point was discussed extensively by (Sekatski *et al.*, 2009, 2010) who showed that any loss of data allows the formulation of a kind of "detection loophole" that impairs the success of the entanglement demonstration. Let's remind that it has been known for at least four decades that a general "detection loophole" exists in the refutation of Local Realistic Theories, and is the source of skepticism about the definitiveness of all experiments dealing with single particle Bell Inequality violations. In facts, as claimed repeatedly by John S. Bell itself, because of the absence of an experimental confirmation of the "fair sampling" assumption or of a plausible equivalent one, all experimental tests of the Bell's Inequality may today interpreted in large areas of the scientific community as merely "good in-

dications” of the real existence of quantum non-locality (Bell, 1987; Greenberger, 1986; Maudlin, 2002). However, it is also well known that the detection loophole can be closed for single particle Bell’s inequality experiments by the adoption of detectors with efficiency as large as $\eta \geq 85\%$ (Eberhard *et al.*, 1993). Quite unfortunately our results show that an even larger value of η is required to demonstrate Micro-Macro entanglement in multiparticle systems. A thorough analysis of the Micro-Macro entanglement was carried out by (Spagnolo *et al.*, 2010c) demonstrating that a priori knowledge of the system that generates the Micro-Macro pair is necessary to exclude a class of separable states that can reproduce the obtained experimental results. In conclusion, the genuine unbiased demonstration of bipartite Micro-Macro entanglement, i.e. in absence of any a priori assumption, is still an open experimental challenge when a very large number M of particles are involved.

4. Effects of coarse-grained measurement

Recently (Raeisi *et al.*, 2011) analyzed the effects of coarse-graining in photon number measurements on the observability of Micro-Macro entanglement that is created by greatly amplifying one photon from an entangled pair. They compared the results obtained for a unitary quantum cloner, which generates Micro-Macro entanglement, and for a measure-and-prepare cloner, which produces a separable Micro-Macro state. Their approach demonstrates that the distance between the probability distributions of results for the two cloners approaches zero for a fixed moderate amount of coarse-graining. Once again, this proves that the detection of Micro-Macro entanglement becomes progressively harder as the system’s size increases (Raeisi *et al.*, 2011).

As alternative approach to demonstrate the Micro-Macro entanglement, (Raeisi, Tittel *et al.*, 2011) proposed a scheme where a photon is first cloned using stim-

ulated parametric down conversion, making many optimal copies, and then the cloning transformation is inverted, regenerating the original photon while destroying the copies. Focusing on the case where the initial photon is entangled with another photon, (Raeisi, Tittel *et al.*, 2011) studied the conditions under which entanglement can be proven in the final state. This proposed experiment would provide a clear demonstration that quantum information is preserved in phase-covariant quantum cloning but again one photon should be lost between the cloning transformation and the following inversion process. The experimental reversion of the optimal quantum cloning and flipping processes has been reported by (Sciarrino *et al.*, 2006). There, the combination of linear and nonlinear optical methods was exploited to implement a scheme that, after the cloning transformation, restores the original input qubit in one of the output channels, by using local measurements, classical communication, and feedforward. This nonlocal method demonstrated how the information on the input qubit can be restored after the cloning process.

5. Hybrid criteria

Very recently (Spagnolo *et al.*, 2011) analyzed a hybrid approach to the experimental assessment of the genuine quantum features of a general system consisting of microscopic and macroscopic parts: Fig.10. They inferred the presence of entanglement by combining dichotomic measurements on a bidimensional system and a phase-space inference through the Wigner distribution associated with the macroscopic component of the state. As a benchmark, the method was adopted to investigate the feasibility of the entanglement demonstration in a bipartite-entangled state composed of a single-photon and a multiphoton field. This analysis shows that, under ideal conditions, maximal violation of a Clauser-Horne-Shimony-Holt inequality is achievable regardless of the number of photons M in the macroscopic part of the state. The problems arising in the detection of entanglement when losses and detection inefficiency are included can be overcome by the use of a hybrid entanglement witness that allows efficient correction for losses in the few-photon regime. This analysis elicits further interest in the identification of suitable test in the high-loss and large-photon-number region and paves the way to an experimentally feasible demonstration of the properties of entanglement affecting a quite interesting class of states lying at the very border between the quantum and the classical domains.

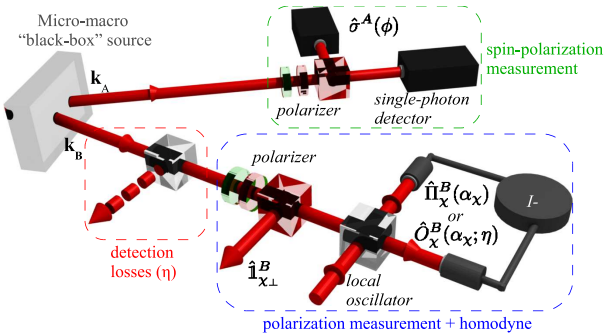


FIG. 10 (Color online) Hybrid non-locality and entanglement test on an optical microscopic-macroscopic state generated by a “black-box”. The single-photon mode \mathbf{k}_A is measured by a polarization detection apparatus, while the multi-photon mode \mathbf{k}_B undergoes both polarization and homodyne measurements.

VII. RESILIENCE TO DECOHERENCE OF THE AMPLIFIED MULTIPARTICLE STATE

In this Section we discuss the resilience to decoherence of the quantum states generated by optical parametric

amplification of a single-photon qubit. The basic tools of this investigation are provided by two coherence criteria expressed by (De Martini *et al.*, 2009a,b). There, the Bures distance (Bures, 1969; Hubner, 1992; Jozsa, 1994):

$$\mathcal{D}(\hat{\rho}, \hat{\sigma}) = \sqrt{1 - \sqrt{\mathcal{F}(\hat{\rho}, \hat{\sigma})}}, \quad (20)$$

where \mathcal{F} is a quantum "fidelity", has been adopted as a measure to quantify: **(I)** the "distinguishability" between two quantum states $\{|\phi_1\rangle, |\phi_2\rangle\}$ and **(II)** the *degree of coherence*, i.e. superposition visibility of their macroscopic quantum superpositions (MQS) $|\phi^\pm\rangle = 2^{-1/2}(|\phi_1\rangle \pm |\phi_2\rangle)$. These criteria were chosen according to the following considerations: **(I)** The distinguishability i.e. the degree of orthogonality, represents the maximum discrimination among two quantum states achievable within a measurement. **(II)** The visibility, between the superpositions $|\phi^+\rangle$ and $|\phi^-\rangle$ depends exclusively on the relative phase of the component states: $|\phi_1\rangle$ and $|\phi_2\rangle$. Consider two orthogonal superpositions $|\phi^\pm\rangle$: $\mathcal{D}(|\phi^+\rangle, |\phi^-\rangle) = 1$. In presence of decoherence the state evolves according to a phase-damping channel \mathcal{E} , the relative phase between $|\phi_1\rangle$ and $|\phi_2\rangle$ progressively randomizes and the superpositions $|\phi^+\rangle$ and $|\phi^-\rangle$ approach an identical fully mixed state leading to: $\mathcal{D}(\mathcal{E}(|\phi^+\rangle), \mathcal{E}(|\phi^-\rangle)) = 0$. The physical interpretation of $\mathcal{D}(\mathcal{E}(|\phi^+\rangle), \mathcal{E}(|\phi^-\rangle))$ as visibility is legitimate insofar as the component states of the corresponding superposition, $|\phi_1\rangle$ and $|\phi_2\rangle$ may be defined, at least approximately, as "pointer states" or "einselected states" (Zurek, 2003). Within the set of the eigenstates characterizing the system under investigation, the pointer states are defined as the ones less affected by the external noise and that are highly resilient to decoherence.

Let's now compare the resilience properties of the different classes of quantum states after the propagation over a lossy channel \mathcal{E} . This one is modelled by a linear beam-splitter (BS) with transmittivity T and reflectivity $R = 1 - T$ acting on a state $\hat{\rho}$ associated with a single BS input mode. Let's first analyze the behaviour of the coherent states and their superpositions. The investigation on the Glauber's states leading to the $\alpha - MQS$'s case (Schleich *et al.*, 1991): $|\Phi_{\alpha\pm}\rangle = \mathcal{N}^{-1/2}(|\alpha\rangle \pm |-\alpha\rangle)$ in terms of the "pointer states" $|\pm\alpha\rangle$ leads to the closed form result: $\mathcal{D}(\mathcal{E}(|\Phi_{\alpha+}\rangle), \mathcal{E}(|\Phi_{\alpha-}\rangle)) = \sqrt{1 - \sqrt{1 - e^{-4R|\alpha|^2}}}$. This one is plotted in Fig.11 (dashed line) as function of the average number of lost photons: $x \equiv R\langle n \rangle$. Note that the value of $\mathcal{D}(\mathcal{E}(|\Phi_{\alpha+}\rangle), \mathcal{E}(|\Phi_{\alpha-}\rangle))$ drops from 1 to 0.095 upon loss of only one photon: $x = 1$. In other words, any superposition of $\alpha - states$. $|\Phi_{\alpha\pm}\rangle = \mathcal{N}^{-1/2}(|\alpha\rangle \pm |-\alpha\rangle)$ exhibits a fast decrease in its coherence, i.e. of its "visibility" and "distinguishability", while the related components $|\pm\alpha\rangle$, i.e. the "pointer states" (Zurek, 2003), remain distinguishable until all photons of the state are depleted by the BS.

Let us now analyze the behaviour of the amplified multiphoton states by a QI-OPA apparatus de-

scribed in the previous Sections. An EPR pair $|\psi^-\rangle = 2^{-1/2}(|H\rangle_A|V\rangle_B - |V\rangle_A|H\rangle_B)$ is generated in a first nonlinear crystal: Figure 6. By analyzing and measuring the polarization of the photon associated with the mode \mathbf{k}_A , the photon on mode \mathbf{k}_B is prepared in the polarization qubit: $|\psi\rangle_B = \cos(\theta/2)|H\rangle_B + e^{i\phi}\sin(\theta/2)|V\rangle_B$. Then, the single photon is injected in the amplifier simultaneously with the strong UV pump beam \mathbf{k}'_P . Let us analyze the two configurations of the apparatus leading, as said, to two different regimes of quantum cloning: the "phase covariant" and the "universal".

A. Phase-covariant optimal quantum cloning machine

We evaluated numerically the *distinguishability* of $\{|\Phi_{PC}^{+,-}\rangle\}$ through the distance $\mathcal{D}(\mathcal{E}(|\Phi_{PC}^+\rangle), \mathcal{E}(|\Phi_{PC}^-\rangle))$: Fig.11. Consider the MQS of the macrostates $|\Phi_{PC}^+\rangle$, $|\Phi_{PC}^-\rangle$: $|\Phi_{PC}^{R/L}\rangle = \frac{\mathcal{N}_\pm}{\sqrt{2}}(|\Phi_{PC}^+\rangle \pm i|\Phi_{PC}^-\rangle)$. Due to the linearity of the amplification process and in virtue of the phase-covariance of the process (De Martini *et al.*, 2009a,b):

$$\mathcal{D}(|\Phi_{PC}^R\rangle, |\Phi_{PC}^L\rangle) = \mathcal{D}(|\Phi_{PC}^+\rangle, |\Phi_{PC}^-\rangle) \quad (21)$$

These equations can be assumed as the theoretical conditions assuring the same behaviour for any quantum MQS state generated by the QI-OPA in the collinear configuration: they identify the equatorial set of the Bloch sphere a privileged resilient to losses Hilbert subspace. The *visibility* of the state $|\Phi_{PC}^{R/L}\rangle$ was evaluated numerically analyzing the Bures distance as a function of x : Figure 11. Note that for small values of x the decay of $\mathcal{D}(x)$ is far slower than for the coherent $\alpha - MQS$ case.

B. Universal optimal quantum cloning machine

Let's now investigate the resilience to decoherence of the MQS generated by the universal optimal quantum cloning machine (Spagnolo *et al.*, 2010a). At variance with the phase-covariant amplifier, the output states do not exhibit any comb structure in their photon number distributions. In agreement with the universality property of the source, the Bures distance between the MQS states $|\Phi_U^{1\psi}\rangle = \cos(\theta/2)|\Phi_U^{1H}\rangle + e^{i\phi}\sin(\theta/2)|\Phi_U^{1V}\rangle$ and $|\Phi_U^{1\psi\perp}\rangle$ is independent of the choice of (θ, ϕ) :

$$\mathcal{D}(\hat{\rho}_U^{1\psi}, \hat{\rho}_U^{1\psi\perp}) = \mathcal{D}(\hat{\rho}_U^{1\psi'}, \hat{\rho}_U^{1\psi'\perp}) \quad (22)$$

for any basis $\{\vec{\pi}_\psi, \vec{\pi}_{\psi'}\}$. The larger symmetry of the latter identifies a larger Hilbert space of macroscopic quantum superpositions resilient to decoherence, corresponding to the complete polarization Bloch sphere. The cost of this larger symmetry is a lower Bures distance in the universal case with respect to the phase-covariant one. This represents an expected trade off in similar cases, e.g. it

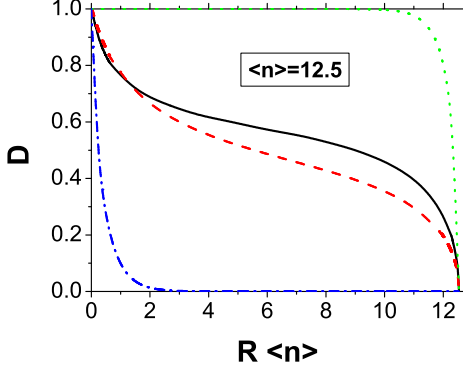


FIG. 11 Bures distance for various classes of MQSs for $\langle n \rangle = 12.5$. The lower blue dash-dotted curve corresponds to $\mathcal{D}(\mathcal{E}(|\phi^+\rangle), \mathcal{E}(|\phi^-\rangle))$, while the green dotted upper curve is relative to the distinguishability $\mathcal{D}(\mathcal{E}(|\alpha^+\rangle), \mathcal{E}(|\alpha^-\rangle))$. The black straight curve corresponds to the MQS generated by phase-covariant cloning $\mathcal{D}(\mathcal{E}(|\Phi_{PC}^+\rangle), \mathcal{E}(|\Phi_{PC}^-\rangle))$ (De Martini *et al.*, 2009a,b), while the red dashed curve corresponds to the universal cloning based MQS $\mathcal{D}(\mathcal{E}(|\Phi_U^+\rangle), \mathcal{E}(|\Phi_U^-\rangle))$ (Spagnolo *et al.*, 2010a).

parallels the well known increase of cloning fidelity due to the reduced size of the Hilbert subspace in the case of phase covariance.

C. Effective size of the multiparticle superposition

Recent experiments on the formation of quantum superposition states in near-macroscopic systems raise the question of how the sizes of general quantum superposition states are to be quantified (Leggett, 2002). The first method to quantify the Cat-size measure was introduced by (Leggett, 1980): the so-called “disconnectivity”. However a closer analysis of the disconnectivity shows that for indistinguishable particles this quantity is large even for no-superposition states, like single-branch Fock states, due to the particle correlations induced by symmetrization.

In the last few years, several criteria have been developed to establish the effective size of macroscopic superpositions. (Dur *et al.*, 2002) investigated state having the form $|\phi_1\rangle^{\otimes M} + |\phi_2\rangle^{\otimes M}$, where the number of subsystems M is very large, but the states of the individual subsystems have large overlap equal to $1 - \epsilon^2$. These authors proposed two different methods for assigning an effective particle number to such states, using ideal Greenberger-Horne-Zeilinger states of the form $|0\rangle^{\otimes M} + |1\rangle^{\otimes M}$ as a standard of comparison. The two methods, based on decoherence and on a distillation protocol, lead to an effective size n of the order of $M\epsilon^2$. The adoption of this criteria to superconducting flux states provides a situation where counting the number of electrons that are involved in the two current carrying the states gives a very

large estimate for the size of the superposition, while a detailed analysis of how many electrons are actually behaving differently in the two branches gives a very different and much smaller value. The Dur, Simon and Cirac criteria has been latter generalized by (Marquardt *et al.*, 2008), which proposed a size measure based on counting how many single-particle operations are needed to map one state component (the “live cat”) into the other one (the “died cat”).

A different approach has been introduced by (Korsbakken *et al.*, 2007) who proposed a measure of size for such superposition states that is based on what measurements can be performed to probe and distinguish the different branches of the macroscopic superposition. This approach allows the comparison of the effective size for superposition states in very different physical systems. Comparison with measure based on analysis of coherence between branches (Leggett, 1980) indicates that this measurement-based measure provide significantly smaller effective superposition sizes. This criteria have been applied to macroscopic superposition states in flux qubits revealing the effective size to be bounded by values in the range of $12 \div 100$ (Korsbakken *et al.*, 2010).

While (Dur *et al.*, 2002) approach could not be applied to the present amplification scheme, (Korsbakken *et al.*, 2007) criteria for effective size can be estimated by exploiting the previous results on the Bures distance between the macro-states. The problem of determining quantum states that can be deterministically discriminated can be directly related to the Bures distance between the involved state (Markham *et al.*, 2008). There it has been shown that the probability of success of the discrimination p_{disc} between two states ρ_1, ρ_2 fulfill the bound $p_{disc}(\rho_1, \rho_2) \leq \mathcal{D}(\rho_1, \rho_2)$. According to Figure 11, the Bures distance $\mathcal{D}(\mathcal{E}(|\Phi_{PC}^+\rangle), \mathcal{E}(|\Phi_{PC}^-\rangle))$ between falls down from 1 to 0.8 as soon as an average of 1 photon is lost. Accordingly the close to perfect discrimination among the states $|\Phi_{PC}^+\rangle$ and $|\Phi_{PC}^-\rangle$ would require to detect almost all particles. This result suggests that according to (Korsbakken *et al.*, 2007) criteria the effective size of the macroscopic quantum superposition is rather limited, analogously to superconducting macro-superposition. On the other side, we should note that the macrostates, $|\Phi^\phi\rangle_B, |\Phi^{\phi^\perp}\rangle_B$ exhibit observables bearing macroscopically distinct average values even in lossy regime with transmittivity T . Precisely, the average number of photons associated with the polarization mode $\vec{\pi}_\phi$ is: $T\bar{m}$ for $|\Phi^{\phi^\perp}\rangle_B$, and $T(3\bar{m} + 1)$ for $|\Phi^\phi\rangle_B$. For the π -mode $\vec{\pi}_{\phi^\perp}$, orthogonal to $\vec{\pi}_\phi$, these values are interchanged among the two states. Hence we tend to agree with (Korsbakken *et al.*, 2007) according to which, that more general measures for comparing the effective size of superposition states in different kinds of physical systems should be developed.

Other approaches have been proposed to quantify macroscopic quantum superposition. First of all (Bjork and Mana, 2004) proposed an operational approach. Their size criterion for macroscopic super-

position states is based on the fact that a superposition presents greater sensitivity in interferometric applications than its superposed constituent states. (Lee and Jeong *et al.*, 2009) proposed to quantify the degree of quantum coherence and the effective size of the physical system that involves the superposition by exploiting quantum interference in phase space. Finally (Shimizu and Miyadera, 2002; Shimizu and Morimae, 2005) proposed an index of macroscopic entanglement based on correlation of local observables on many sites in macroscopic quantum systems.

VIII. WIGNER - FUNCTION THEORY

Let us now address the problem of providing a complete quantum phase-space analysis able to recognize the persistence of the QI-OPA properties in a decohering environment. Among the different representation of quantum states in the continuous-variables space (Cahill and Glauber, 1969), the Wigner quasi-probability representation has been widely exploited to investigate non-classical properties, such as squeezing (Walls and Milburn, 1995) and EPR non-locality (Banaszek and Wódkiewicz, 1998). In particular, the presence of negative quasi-probability regions has been considered as a consequence of the quantum superposition of distinct physical states (Bartlett, 1944). By the way, the negativity of the Wigner function is not the only parameter that allows to estimate the non-classicality of a certain state. For instance, the squeezed vacuum state (Walls and Milburn, 1995) presents a positive W -representation, while its properties cannot be described by the laws of classical physics. Furthermore, recent papers have shown that the Wigner function of an EPR state provides direct evidence of its non-local character (Banaszek and Wódkiewicz, 1998; Cohen, 1997), while being completely-positive in all the phase-space.

In order to investigate the properties of the output field of the QI-OPA device in details, we analyze the quasi-probability distribution introduced by Wigner (Wigner, 1932) for the amplified field. The Wigner function is defined as the Fourier transform of the symmetrically-ordered characteristic function $\chi(\eta)$ of the state described by the general density matrix $\hat{\rho}$

$$\chi(\eta) = \text{Tr} [\hat{\rho} \exp(\eta \hat{a}^\dagger - \eta^* \hat{a})] \quad (23)$$

The associated Wigner function

$$W(\alpha) = \frac{1}{\pi^2} \int \exp(\eta^* \alpha - \eta \alpha^*) \chi(\eta) d^2 \eta \quad (24)$$

exists for any $\hat{\rho}$ but is not always positive definite and, consequently, can not be considered as a genuine probability distribution.

The properties of the multiphoton system have been investigated (Spagnolo *et al.*, 2009) in phase-space by a Wigner quasi-probability function analysis when the

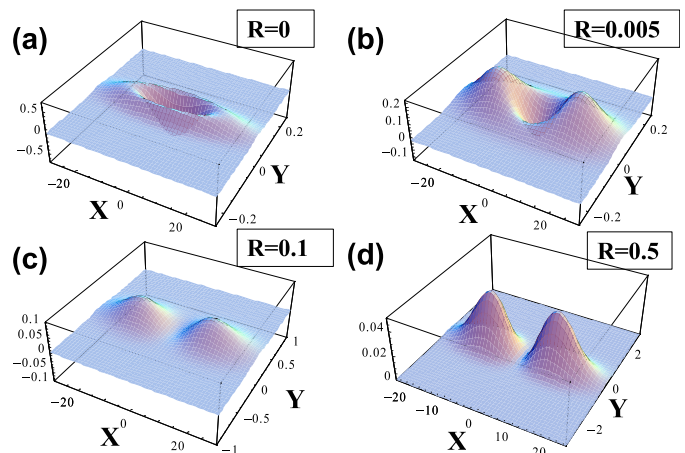


FIG. 12 Wigner function of a single-photon amplified state in a single-mode degenerate OPA for $g = 3$. (a) ($R=0$) Unperturbed case. (b) ($R=0.005$) For small reflectivity, the Wigner function remains negative in the central region. (c) ($R=0.1$) The Wigner function progressively evolve in a positive function in all the phase-space. (d) ($R=0.5$) Transition from a non-positive to a completely positive Wigner function (Spagnolo *et al.*, 2009).

fields propagate over a lossy channel. Fig.12-a reports the ideal case, in absence of losses, showing the presence of peculiar quantum properties such as squeezing and a non-positive W -representation. Then, by investigating the resilience to losses of QI-OPA amplified states in a lossy configuration, the persistence of the non-positivity of the Wigner function was demonstrated in a certain range of the *system-environment* interaction parameter R . This behaviour can be compared with the one shown by the $|\alpha\rangle$ states MQS, which features a non-positive W -representation in the same interval of R . The more resilient structure of the QI-OPA amplified states has been enlightened by their slower decoherence rate, represented by both the slower decrease in the negative part of the Wigner function and by the behavior of the Bures distance between orthogonal macrostates (Spagnolo *et al.*, 2009). Since the negativity of the W -representation is a sufficient but not a necessary condition for the non-classicality of any physical system, future investigations should be aimed at the regime of decoherence in cases in which the Wigner function is completely positive, analyzing by different criteria the presence of the related quantum properties of the system.

IX. GENERATION OF MACRO-MACRO ENTANGLED STATES

One of the main challenges for an experimental test of entanglement in systems of large size is the realization of suitable criteria for the detection of entanglement in bipartite macroscopic systems. A large effort has been devoted in the last few years in this direction

(Horodecki *et al.*, 2009). Some criteria, such as the partial transpose criterion developed by (Horodecki *et al.*, 1996; Peres, 1997), require the tomographic reconstruction of the density matrix, which from an experimental viewpoint is generally highly demanding for system composed by a large number M of particles. However, the complete reconstruction of the state can be avoided by the “entanglement witness” method consisting of a class of tests where only few significant local measurements are performed. For bipartite systems with large M , this approach has been applied via collective measurements on the state. Within this context, Duan *et al.* proposed a general criterion based on measurements on “continuous variables” observables (Braunstein and van Loock, 2005; Duan *et al.*, 2000). This general criterion was subsequently applied to the quantum extension of the Stokes parameters in order to obtain an entanglement bound for such type of variables (Korolkova and Leuchs, 2002; Korolkova *et al.*, 2002; Schnabel *et al.*, 2003). Other approaches have been developed based on spin variables (Simon and Bouwmeester, 2003) or pseudo-Pauli operators (Chen *et al.*, 2002). An experimental application of this criteria based on collective spin measurements has been performed in a bipartite system consisting by separate two gas samples (Julsgaard *et al.*, 2001).

The main experimental problem for such observations arises from the requirement of attaining a sufficient isolation of the quantum system from its environment, i.e., from the decoherence process (Zurek, 2003). An alternative approach to explain the quantum-to-classical transition has been recently proposed by Kofler and Brukner, along an idea earlier discussed by Bell, Peres and Mermin (Peres, 1993). They considered the emergence of classical physics in systems of increasing size *within* the domain of quantum theory (Kofler and Brukner, 2007). Precisely, they focused on the limits of the observability of quantum effects in macroscopic objects, showing that, for large systems, macrorealism arises under coarse-grained measurements. However, some counterexamples to such modellization were found later by the same authors: some non classical Hamiltonians violate macrorealism in spite coarse-grained measurements (Kofler and Brukner, 2008). Therefore the problem of the resolution within the measurement process appears to be a key ingredient in the understanding the limits of the quantum behavior of macroscopic physical systems and the quantum-to-classical transition. In a recent paper Jeong *et al.* contributed to the investigation about the possibility of observing the quantum features of a system under fuzzy measurement, by finding that extremely-coarse-grained measurements can still be useful to reveal the quantum world where local realism fails (Jeong *et al.*, 2009).

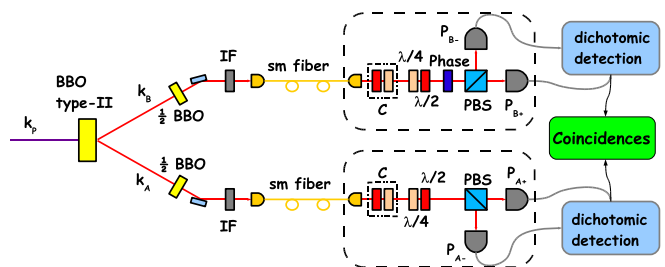


FIG. 13 Setup for the generation and detection of a bipartite macroscopic field. The high laser pulse on mode \mathbf{k}_P excites a type-II noncollinear source in the high gain regime ($g = 3.5$). The two spatial mode \mathbf{k}_A and \mathbf{k}_B are spectrally and spatially selected by interference filters (IF) and single mode fibers. After fiber compensation (C), the two modes are analyzed in polarization and detected by four photomultipliers (Vitelli *et al.*, 2010c).

A. Macroscopic quantum state based on high gain spontaneous parametric down-conversion

Let us consider, once again, an optical parametric amplifier working in a high gain regime. The radiation field under investigation is the quantum state obtained by spontaneous parametric down-conversion (SPDC) (Eisenberg *et al.*, 2004; Kwiat *et al.*, 1995b), whose interaction Hamiltonian is: $\mathcal{H}_U = i\hbar\chi \left(\hat{a}_\pi^\dagger \hat{b}_{\pi_\perp}^\dagger - \hat{a}_{\pi_\perp}^\dagger \hat{b}_\pi^\dagger \right) + \text{H.c.}$

The output state reads (Caminati *et al.*, 2006b; Eisenberg *et al.*, 2004; Simon and Bouwmeester, 2003):

$$|\Psi^-\rangle = \frac{1}{C^2} \sum_{n=0}^{\infty} \Gamma^n \sqrt{n+1} |\psi_n^-\rangle \quad (25)$$

with

$$|\psi_n^-\rangle = \frac{1}{\sqrt{n+1}} \sum_{m=0}^n (-1)^m |(n-m)\pi, m\pi_\perp\rangle_A |m\pi, (n-m)\pi_\perp\rangle_B \quad (26)$$

The output state can be written as the weighted coherent superposition of singlet spin- $\frac{n}{2}$ states $|\psi_n^-\rangle$.

This source has been adopted in many experiments, at different gain regimes. First, (Kwiat *et al.*, 1995b) exploited the polarization singlet-state emitted in the single-pair regime to test the violation of Bell’s inequalities. Further work demonstrated experimentally the four-photon entanglement in the second-order emission state of the SPDC source, by detecting the four-fold coincidences after the two output modes of the source were coupled to two 50-50 beam-splitters (BS) (Eibl *et al.*, 2003). Moreover, a generalized non-locality test was also successfully performed with this configuration (Weinfurter and Zukowski, 2001). Later, a similar scheme was adopted by Wieczorek *et al.* to experimentally generate an entire family of four-photon entangled states (Wieczorek *et al.*, 2008).

1. Non-separable Werner states

As previously mentioned, the presence of polarization-entanglement in the multi-photon states up to $M = 12$ photons was experimentally proved by investigating the high loss regime in which at most one photon per branch was detected (Caminati *et al.*, 2006a; Eisenberg *et al.*, 2004). This approach consisted of the generation of a multiphoton state followed by a strong attenuation on both output branches of the SPDC scheme, in order to “extract” a correlated couple of photons, one for each branch: Figure 13. The method presents several advantages: first, the techniques for single-photon detection and characterization can be adopted. Second, it models the effect of loss associated with any communication process on a multiphoton entangled state.

The density matrix of the two-photon state has been investigated by theory and experiment (Caminati *et al.*, 2006b). The state given by Eq.(25), is stochastically attenuated by a conventional beam-splitter model that simulates the propagation over a lossy channel. Then the density matrix of the two-photon state generated by postselection is expressed by:

$$\rho_{SPDC}^{HG} = \begin{pmatrix} \frac{1-p}{4} & 0 & 0 & 0 \\ 0 & \frac{1+p}{4} & -\frac{p}{2} & 0 \\ 0 & -\frac{p}{2} & \frac{1+p}{4} & 0 \\ 0 & 0 & 0 & \frac{1-p}{4} \end{pmatrix} \quad (27)$$

with singlet weight $p = \frac{1}{2\Gamma^2+1}$ and $\tilde{\Gamma} = (1-\eta) \tanh g$. We note that the density matrix ρ_{SPDC}^{HG} is a Werner state, i.e., a weighted superposition of a maximally entangled singlet state with a fully mixed state (Werner, 1989). As it is well known, the Werner states play a paradigmatic role in quantum information; as they determine a family of mixed states including both entangled and separable states (Barbieri *et al.*, 2004). They model the decoherence process occurring on a singlet state traveling along a noisy channel, and hence they are adopted to investigate the distillation and concentration processes. Furthermore, depending on the singlet weight they can exhibit either entanglement and violation of Bell inequalities, or only entanglement, or separability. In the limit $\eta \rightarrow 0$ the above equation gives: $\tilde{\Gamma} = \tanh g \approx 1$, for large g . In the hypothesis of very high losses, the singlet weight $p \geq \frac{1}{3}$ approaches the minimum value $\frac{1}{3}$. Since the condition $p > \frac{1}{3}$ implies the non-separability condition for a general Werner state, the two-photon state is entangled for any large value of g . Figure 13 shows the result of the theory together with the experimental demonstration of bipartite entanglement for: $M \leq 12$.

2. Quantum-to-classical transition by dichotomic measurement

We are now interested in analyzing the behavior of the system above considered when the number of generated photons is increased and the system undergoes a

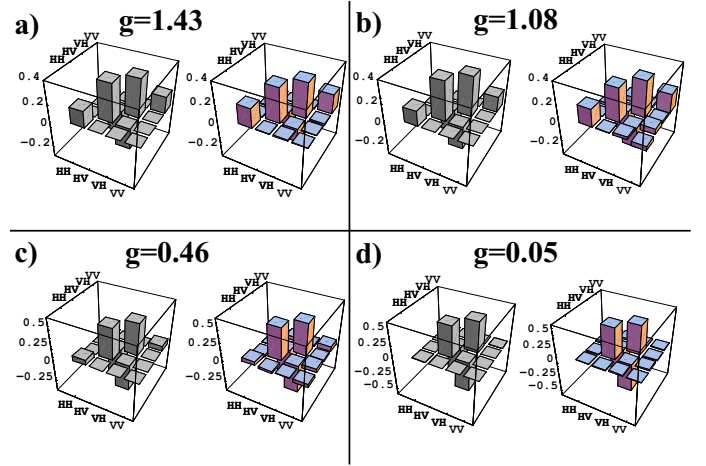


FIG. 14 Theoretical (left plot) and experimental(right plot) density matrices ρ_{SPDC}^{HG} for different gain values. The experimental density matrices have been reconstructed by measuring 16 two qubits observables (Caminati *et al.*, 2006a).

fuzzy dichotomic measurement on the overall state, in which the generated particles cannot be addressed singularly. As shown by (Chen *et al.*, 2002), the demonstration of non-locality in a multiphoton state produced by a non-degenerate optical parametric amplifier would require the experimental application of “parity operators”, with a detector efficiency: $\eta = 1$. On the other hand, the estimation of a coarse grained quantity through collective measurements as suggested by (Portolan *et al.*, 2006), would miss the underlying quantum structure of the generated state, introducing elements of local realism even in presence of strong entanglement and in absence of decoherence. A theoretical investigation on a multiphoton system generated by parametric down conversion was carried out by Reid and coworkers (Reid *et al.*, 2002). They analyzed the possibility of testing the violation of Bell’s inequality by performing dichotomic measurement on the multiparticle quantum state. Precisely, in analogy with the spin formalism and the O-Filter discrimination, they proposed to compare the number of photons polarized “up” with the number of photons polarized “down” at the exit of the amplifier: a dichotomic measurement on the multiphoton state. In such a way a small violation of the multiparticle Bell’s inequality can be revealed even in presence of losses and of the quantum inefficiency of detectors. Once again, the violation decreases very rapidly for an increasing number M of the generated photons. In a recent paper (Bancal *et al.*, 2008) have discussed different techniques for testing the Bell’s inequality violation in multipair scenarios by performing a global measurement, in either Alice’s and Bob’s sites. According to their theory, the photon pairs were classified as “distinguishable”, i.e. independent, or “indistinguishable”, i.e. belonging to the same spatial and temporal mode. They found that while the state of indistinguishable pairs results more entangled, the state of independent pairs ap-

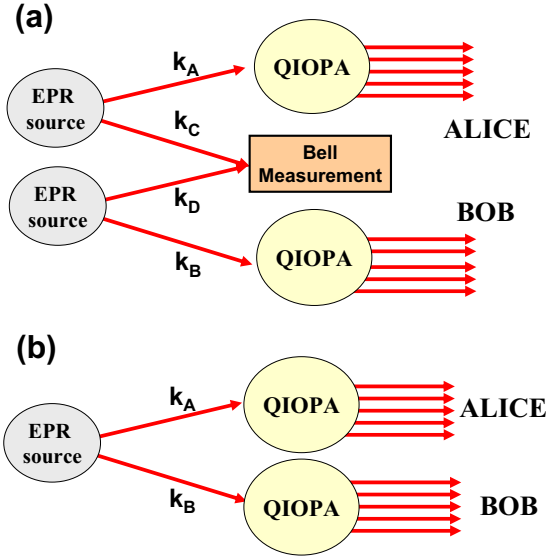


FIG. 15 Implementation of macro-macro entanglement (a) via entanglement swapping on two QI-OPA (b) through two optical parametric amplifiers (De Martini, 2010).

pears to be more nonlocal.

The possibility of observing quantum correlations in macroscopic systems through dichotomic measurement, by addressing two different measurement schemes, based on different dichotomization processes has recently addressed by (Vitelli *et al.*, 2010c). More specifically, the persistence of non-locality in a spin- $\frac{n}{2}$ singlet state with increasing size has been investigated by studying the change in the correlations form as n increases, both in the ideal case and in presence of losses. Two different types of dichotomic measurements on multiphoton states were considered: the orthogonality filtering and the threshold detection. Numerical simulation showed that the interference fringe-patterns for singlet- $\frac{n}{2}$ states exhibit a transition from the sinusoidal pattern of the spin- $\frac{1}{2}$ into a quasi-linear pattern by increasing the number of photons associated with the spin state. According to this behavior a progressive decrease of the amount of the violation is observed, as earlier predicted by (Bancal *et al.*, 2008; Reid *et al.*, 2002). All these results show that the dichotomic fuzzy measurements lack of the necessary resolution to characterize such states. They also show, once again, how problematic is the experimental demonstration of quantum non-locality of states with very large M .

B. Macroscopic quantum state by dual amplification of two-photon entangled state

The amplification schemes illustrated by the Figures 1 a), b), c) could be upgraded in order to achieve an entangled macro-macro system showing nonlocality features (De Martini, 2010). Such scheme could even exploit

an entanglement swapping protocol as shown in Fig.8 a)(Pan *et al.*, 1998; Żukowski *et al.*, 1993). There the final entangled state is achieved through a standard intermediate Bell measurement carried out on the single photon states. A similar process has been suggested in several different contexts, e.g. to entangle micromechanical oscillators (Pirandola *et al.*, 2006). As an alternative approach, the single photon states on mode k_A and k_B could be amplified by two independent QI-OPA's :Fig.8 b). The resulting Macro-Macro scenario would be an interesting platform to perform loophole free Bell inequalities.

An open question is how to perform an entanglement or/and non-locality test on the Macro-Macro states. Indeed, analogously to the Micro-Macro scenario, a coarse-grained measurement resolution would be requested. To overcome this challenge, it has been proposed to manipulate multiphoton quantum states obtained through optical parametric amplification by performing a measurement on a small portion of the output light field. (Vitelli *et al.*, 2010a) analyzed in details how the quantum features of the Macro-states are modified by varying the amount of extracted information and considered the best strategy to be adopted at the final measurement stage. At last it was found that the scheme does not allow one to violate any multiphoton Bell's inequality in absence of auxiliary assumptions.

A similar investigation on the preprocessing of quantum macroscopic states of light generated by optimal quantum cloners in the presence of classical detection has been carried out by (Stobinska *et al.*, 2011). These Authors proposed a filter that selects two-mode high number Fock states whose photon-number difference exceeds a certain value. This filter improves the distinguishability of some states by preserving the quantum macroscopic superposition (Stobinska *et al.*, 2011b). It is still an open question whether this filter can be efficiently implemented and whether it can lead to a genuine non-locality test.

X. INTERACTION WITH A BOSE-EINSTEIN CONDENSATE

In recent years a great deal of interest has been attracted by the ambitious challenge of creating a macroscopic quantum superposition of a massive object by an entangled opto-mechanical interaction of a tiny mirror with a single photon trapped within a Michelson interferometer (Marshall *et al.*, 2003), This would lead to another realization of the well known 1935 argument by Schrödinger (Schrödinger, 1935). A similar scheme could be considered which is based on the nonresonant scattering by a properly shaped *multi-atom* Bose-Einstein condensate (BEC) of the *multi-photon* state $|\Phi\rangle$ generated by a high-gain quantum-injected optical parametric amplifier (QI-OPA) described at Chapter II of the present article. Light scattering from BEC structures has been

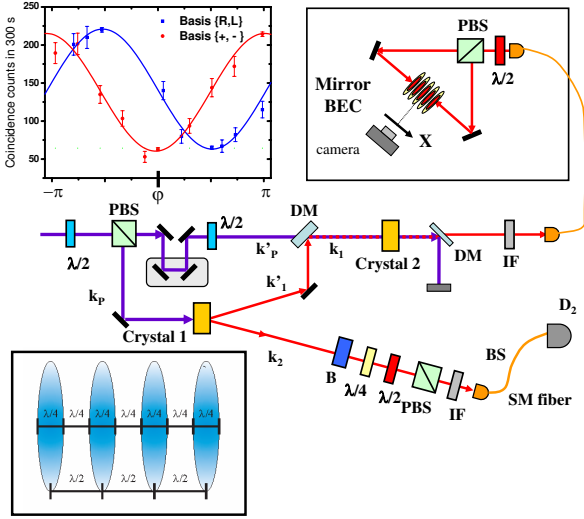


FIG. 16 Layout of the QI-OPA and Mirror BEC experimental apparatus. The upper left inset shows the interference patterns detected at the output of the PBS shown in the UR-Inset for two different measurement basis $\{+, -\}$ and $\{L, R\}$. Alternating slabs of condensate and vacuum are shown in the lower left inset (De Martini *et al.*, 2010)

adopted so far to enhance their non-linear macroscopic properties in super-radiance experiments (Inouye, 1999), to show the possibility of matter wave amplification (Kozume, 1999) and non-linear wave mixing (Deng *et al.*, 1999). The new scheme, represented by Fig.16, would result in a joint atom-photon Micro-Macro state entangled by momentum conservation. The resulting physical effect would consist of the mechanical motion of a high reflectivity optical multilayered Bragg-shaped mirror, referred to as a "Mirror-BEC", driven by the exchange of linear momentum with a photonic Macrostate $|\Phi\rangle$.

The layout in Figure 16 shows a QI-OPA system identical to the one represented in Figure 1 c). The interfering polarization macrostates belonging to the quantum superposition (MQS): $|\Phi\rangle = 2^{-\frac{1}{2}}(|\Phi^\phi\rangle + |\Phi^{\phi^\perp}\rangle)$ generated over mode k_2 are selected by a polarizing beam splitter and drive along the X-axis the mechanical motion of the Mirror-BEC. Precisely, the displacements along the two opposite directions parallel to the X-axis are driven respectively by the orthogonal polarizations: $|\Phi^\phi\rangle$ and $|\Phi^{\phi^\perp}\rangle$. Since these states are found to be entangled with the far apart single-photon emitted over the mode k_2 , the same entanglement property can be transferred to the position-Macrostate of the optically-driven Mirror-BEC. The discussion in Section V dealing with the entanglement processes can be extended to the present more complex opto-mechanical configuration.

XI. APPLICATIONS: FROM SENSING TO RADIOMETRY

A. Quantum sensing

The aim of quantum sensing is to develop strategies able to extract from a system the maximum amount of information with a minimal disturbance. The possibility of performing precision measurements by adopting quantum resources can increase the achievable precision going beyond the semiclassical regime of operation (Giovannetti *et al.*, 2004, 2006; Helstrom, 1976). In the case of interferometry, this can be achieved by the use of the so-called N00N states, which are quantum mechanical superpositions of just two terms, corresponding to all the available photons N placed in either the signal arm or the reference arm of the interferometer. The use of N00N states can enhance the precision in phase estimation to $1/N$, thus improving the scaling of the achievable precision with respect to the employed resources (Boto *et al.*, 2000; Dowling, 2008). This approach can have wide applications for minimally invasive sensing methods acting on quantum states. Nevertheless, these states result extremely fragile under unavoidable losses and decoherence (Gilbert and Weinstein, 2008). For instance, a sample, whose phase shift is to be measured, generally introduce attenuation. Since the quantum-enhanced modes of operations are generally very fragile the impact of environmental effects can be much more harmful than in semiclassical schemes by destroying completely the quantum benefits (Rubin and Kaushik, 2007; Shaji and Caves, 2007). This scenario explains why the overcoming the negative effects of the realistic environments is the main challenge of the technology of quantum sensing. Very recently, the theoretical and experimental engineering of quantum states of light has attracted much attention, leading to the best possible precision in optical two-mode interferometry, even in presence of experimental imperfections (Demkowicz-Dobrzanski *et al.*, 2009; Dorner *et al.*, 2009; Huver *et al.*, 2008; Kacprowicz *et al.*, 2009; Lee *et al.*, 2009; Maccone and De Cillis, 2009).

Recently (Vitelli *et al.*, 2010b) reported an hybrid approach based on a high gain optical parametric amplifier operating for any polarization state in order to transfer quantum properties of different microscopic quantum states in the macroscopic regime. By performing the amplification process of the microscopic probe after the interaction with the sample, it is possible to overcome the detrimental effects of losses on the phase measurement which affects the single photon state following the test on the sample. This approach may be adopted in a minimally invasive scenario where a fragile sample, such as biological system requires a minimum amount of test photons in order to prevent damages. The action of the amplifier, i.e. the process of optimal phase covariant quantum cloning, is to amplify the phase information which

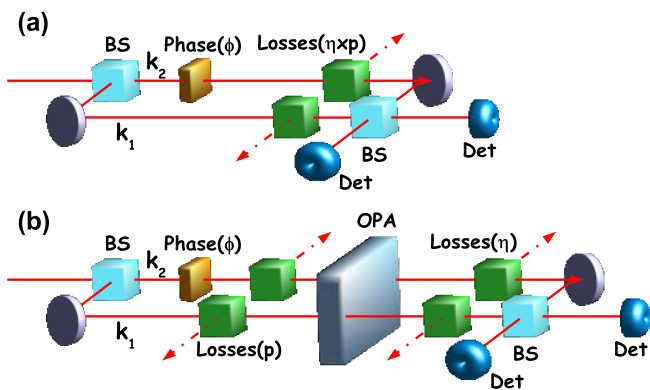


FIG. 17 Scheme for the phase measurement. (a) Interferometric scheme adopted to estimate the phase (ϕ) introduced in the mode k_2 . (b) Interferometric scheme adopting a single photon and the optical parametric amplifier: the amplification of the single photon state is performed before dominant losses (Vitelli *et al.*, 2010b).

is codified in a single photon into a large number of particles. Such multiphoton states exhibit a high resilience to losses, as shown by (De Martini *et al.*, 2009a,b, 2008), and can be manipulated by exploiting a detection scheme which combines features of discrete and continuous variables. The effect of losses on the macroscopic field consists of the reduction of the detected signal and not in the complete cancellation of the phase information as in the single photon probe case, thus improving the achievable sensitivity. This improvement consists in a constant enhancement $K(g)$ of the sensitivity, depending on the amplifier gain g . Hence, the sensitivity scales as \sqrt{N} , where N is the number of photons testing the sample, but the effect of the amplification process reduces the detrimental effect of losses by a factor proportional to the number of generated photons. Within this framework recently (Escher *et al.*, 2011) derived the general bounds on the adoption of quantum metrology in the presence of decoherence are obtained.

B. Quantum radiometry

Radiometry is the science of measuring the electromagnetic radiation. The available technologies in this field can operate either in the relative high power regime or in the photon-counting regime based on the correlations of quantum fields. Very recently a sophisticated radiometer apparatus has been devised that works over a broad range of powers: from the single photon level, up to several tens of nW, i.e. from the quantum regime to the classical regime (Sanguinetti *et al.*, 2010). In fact, such system exploits the process of optimal quantum cloning and is able to provide an absolute measure of spectral radiance by relying on a particular aspect of the quantum-to-classical transition: as the number of information carriers (pho-

tons) grows, so does the cloning fidelity. Sanguinetti *et al.* have shown that the fidelity of cloning can be used to produce an absolute power measurement with an uncertainty limited only by the uncertainty of a relative power measurement. They provided a convincing demonstration of this scheme by an all-fiber experiment at telecom wavelengths, by achieving an accuracy of 4%, a figure that can be easily improved by a dedicated metrology laboratory (Fasel *et al.*, 2002).

XII. CONCLUSIONS AND PERSPECTIVES

In this paper we have reviewed several protocols and related experiments centered on the process of nonlinear amplification of single photon quantum states. A large part of the investigation focused on the new protocol of quantum information, viz. the "quantum injected" version of the optical parametric amplification (OPA), by which a single photon, encoded as a Micro-qubit, "triggers" by a QED process the generation of an in principle unlimited number M of photons, i.e. a Macro-qubit, carrying a large portion of the information associated with the trigger particle. The highly seminal character of the new protocol opened the way to the discovery, the realization and the development of novel scientific methods and applications of fundamental and technical relevance. The quantum information protocols today generally referred to as "quantum cloning", "quantum U-NOT", "macroscopic quantum superposition" (MQS), "Micro-Macro entanglement", "quantum reversion", "quantum-to-classical transition" were amongst the paradigmatic outcomes of the overall endeavour reported in this article, lasting more than one decade. In particular, the QI-OPA method was instrumental for the first experimental realization of the "quantum-cloning" process in several multiparticle regimes. This process was further thoroughly investigated leading to the discovery of the U-NOT theorem, of the quantum reversion protocol and to the first experimental test of the "no signalling theorem". In this connection, the unexpected result of the experiment was that the impossibility of "faster than light communication", i.e. the according to Abner Shimony "peaceful co-existence" between Special Relativity and quantum mechanics, rests of the high-order correlations affecting the particles generated by a cloning machine.

A large part of the investigation focused on the realization via quantum cloning of the Macroscopic Quantum Superposition (MQS) process, which is related to the outstanding quantum-to-classical transition paradigm implied by the celebrated "*Schrödinger's Cat*" argument (Schrödinger, 1935). The realization of the MQS process consisting of a large number of particles $M \geq 10^3$ was experimentally demonstrated, in a *non-entangled* configuration, by detection of the sinusoidal phase dependence of the interference fringe patterns generated at the output of the apparatus. However the

bipartite Micro-Macro entanglement could be demonstrated only for a reduced number of particles, $M \preceq 12$ owing to the existence of a "detection loophole" whose detrimental effect increases with M . A most interesting feature the adopted MQS scheme was found to consist of its resilience to any externally driven de-coherence process: this allowed to carry out the entire research at $T = 300^\circ K$. Accordingly, a large emphasis has been given to an extended theoretical analysis aimed at the understanding this phase-impairing process affecting all multiparticle systems. The extension of the quantum-cloning argument to a novel Macro-Macro regime and the mechanical coherent interaction of a multi-photon MQS system with a multi-atom BEC condensate were considered as proposals towards further research on the foundations of Quantum Mechanics.

Concerning the investigation on quantum-to-classical transition a set of entanglement criteria for bipartite systems of a large number of particles were introduced and analyzed in details. In particular, a specific joint Micro and Macro-scopic system based on optical parametric amplification of an entangled photon pair was addressed. Their potential applications of fundamental and technical relevance in different contexts were analyzed, e.g. the realization of non-locality tests, quantum metrology, quantum sensing and, as an open challenge for future research, the process of "pre-selection", i.e. the establishment of efficient strategies able to generate and wisely manipulate multiphoton states by performing measurements on a small portion of the output field (Vitelli *et al.*, 2010a). Precisely, within the Macro-Macro nonlocality test, the aim was to understand how the features of the Macro-qubit in the high-loss and large-photon-number regime are modified by varying the amount of extracted information and then to devise the best strategy to be adopted at the final measurement stage. In facts, the proposed pre-selection method, the simplest one based on the dichotomic measurement of the reflected part of the wave-function in two different bases did not allow to violate a Bell's inequality. At last a more general approach to the Micro-Macro entanglement problem, based on single photon-continuous variables hybrid methods, was introduced (Spagnolo *et al.*, 2011). All these novel criteria and methods were considered and compared in the context of the existing literature in the field.

In summary, we do believe that the extended theoretical and experimental investigation outlined by the present article can contribute to open new paths of research either by stimulating the discovery of efficient theorems and protocols of quantum information, and, on the more fundamental side, by shedding new light on the still uncertain border existing between the "classical" and the "quantum" aspects of Nature.

Acknowledgments

We would like to thank Nicolò Spagnolo, Chiara Vitelli, Nicolas Gisin, Christoph Simon, Pawel Horodecki for interesting and enlightening discussions. This work was supported by FIRB-Futuro in Ricerca (HYTEQ).

References

- Bae, J., and A. Acín, 2006, *Phys. Rev. Lett.* **97**, 030402.
- Banaszek, K., and K. Wódkiewicz, 1998, *Phys. Rev. A* **58**(6), 4345.
- Bancal, J. D., C. Branciard, N. Brunner, N. Gisin, S. Popescu, and C. Simon, 2008, *Phys. Rev. A* **78**, 062110.
- Barbieri, M., F. De Martini, G. Di Nepi, and P. Mataloni, 2004, *Phys. Rev. Lett.* **92**(17), 177901.
- Bartlett, M. S., 1944, *Proc. Cambridge Philos. Soc.* **41**, 71.
- Bechmann-Pasquinucci, H., and N. Gisin, 1999, *Phys. Rev. A* **59**(6), 4238.
- Bell, J.S., 1987, *Speakable and Unsayable in Quantum Mechanics* (Cambridge University Press).
- Bjork, G., P.G.L. Mana, 2004, *J. Opt. B: Quantum Semiclass. Opt.* **69**, 429.
- Blinov, B., D. Moehring, L.-M. Duan, , and C. Monroe, 2004, *Nature (London)* **428**, 153.
- Boto, A. N., P. Kok, D. S. Abrams, S. L. Braunstein, C. P. Williams, and J. P. Dowling, 2000, *Phys. Rev. Lett.* **85**, 2733.
- Bovino, F., F. De Martini, and M. V., 1999, arXiv:quant-ph/9905048 .
- Boyd, R., 2008, *Nonlinear Optics* (Academic, NY.).
- Braunstein, S. L., and P. van Loock, 2005, *Rev. Mod. Phys.* **77**, 513.
- Bruß, D., M. Cinchetti, G. Mauro D'Ariano, and C. Macchiavello, 2000, *Phys. Rev. A* **62**(1), 012302.
- Bruß, D., D. P. Di Vincenzo, A. Ekert, C. A. Fuchs, C. Macchiavello, and J. A. Smolin, 1998, *Phys. Rev. A* **57**, 2368.
- Bruss, D., A. Ekert, and C. Macchiavello, 1998, *Phys. Rev. Lett.* **81**(12), 2598.
- Bures, D., 1969, *Trans. Am. Math. Soc.* **135**, 199.
- Buzek, V., S. L. Braunstein, M. Hillery, and D. Bruß, 1997, *Phys. Rev. A* **56**(5), 3446.
- Buzek, V., and M. Hillery, 1996, *Phys. Rev. A* **54**, 1844.
- Buzek, V., and M. Hillery, 1998, *Phys. Rev. Lett.* **81**(22), 5003.
- Buzek, V., M. Hillery, and R. F. Werner, 1999, *Phys. Rev. A* **60**(4), R2626.
- Cahill, K. E., and R. J. Glauber, 1969, *Phys. Rev.* **177**, 1882.
- Caminati, M., F. De Martini, R. Perris, F. Sciarrino, and V. Secondi, 2006a, *Phys. Rev. A* **74**(6), 062304.
- Caminati, M., F. De Martini, R. Perris, F. Sciarrino, and V. Secondi, 2006b, *Phys. Rev. A* **73**(3), 032312.
- Caminati, M., F. De Martini, and F. Sciarrino, 2006c, *Laser Physics* **16**, 1551.
- Cerf, N., and J. Fiurasek, 2006, *Progress in Optics* **49**, 455.
- Chen, Z.-B., J.-W. Pan, G. Hou, and Y.-D. Zhang, 2002, *Phys. Rev. Lett.* **88**, 040406.
- Chou, C. W., H. de Riedmatten, D. Felinto, S. V. Polyakov, S. J. van Enk, and H. J. Kimble, 2005, *Nature* **438**, 828.
- Cohen, O., 1997, *Phys. Rev. A* **56**, 3484.
- D'Ariano, G. M., and C. Macchiavello, 2003, *Phys. Rev. A* **67**(4), 042306.

- De Angelis, T., E. Nagali, F. Sciarrino, and F. De Martini, 2007, Phys. Rev. Lett. **99**, 193601.
- De Martini, F., 1998a, Phys. Rev. Lett. **81**, 2842.
- De Martini, F., 1998b, Phys. Lett. A **250**, 15.
- De Martini, F., 2010, Foundations of Physics , doi:10.1007/s10701.
- De Martini, F., V. Buzek, F. Sciarrino, and C. Sias, 2002, Nature **419**, 815.
- De Martini, F., V. Mussi, and F. Bovino, 2000, Optics Communications **179**, 581.
- De Martini, F., D. Pelliccia, and F. Sciarrino, 2004, Phys. Rev. Lett. **92**, 067901.
- De Martini, F., and F. Sciarrino, 2005, Progr. Quantum Electron. **29**, 165.
- De Martini, F., F. Sciarrino, and V. Secondi, 2005, Phys. Rev. Lett. **95**, 240401.
- De Martini, F., F. Sciarrino, and N. Spagnolo, 2009a, Phys. Rev. Lett. **103**, 100501.
- De Martini, F., F. Sciarrino, and N. Spagnolo, 2009b, Phys. Rev. A **79**, 052305.
- De Martini, F., F. Sciarrino, and C. Vitelli, 2008, Phys. Rev. Lett. **100**, 253601.
- De Martini, F., F. Sciarrino, C. Vitelli, and F. S. Cataliotti, 2010, Phys. Rev. Lett. **104**, 050403.
- de Riedmatten, H., J. Laurat, C. W. Chou, E. W. Schomburg, D. Felinto, and H. J. Kimble, 2006, Phys. Rev. Lett. **97**, 113603.
- Demkowicz-Dobrzanski, R., 2005, Phys. Rev. A **71**(6), 062321.
- Demkowicz-Dobrzanski, R., U. Dorner, B. Smith, J. Lundeen, W. Wasilewski, K. Banaszek, and I. Walmsley, 2009, Phys. Rev. A **80**, 013825.
- Deng, L., E. W. Hagley, J. Wen, M. Trippenbach, Y. Band, P. S. Julienne, J. E. Simsarian, K. Helmerson, S. L. Rolston, and W. D. Phillips, 1999, Nature **398**, 218.
- Derka, R., V. Buzek, and A. K. Ekert, 1998, Phys. Rev. Lett. **80**, 1571.
- Dieks, D., 1982, Physics Letters A **92**, 271.
- Dorner, U., R. Demkowicz-Dobrzanski, B. J. Smith, J. S. Lundeen, W. Wasilewski, K. Banaszek, and I. A. Walmsley, 2009, Phys. Rev. Lett. **102**, 040403.
- Dowling, J. P., 2008, Contemp. Phys. **49**, 125.
- Duan, L.-M., G. Giedke, J. I. Cirac, and P. Zoller, 2000, Phys. Rev. Lett. **84**, 2722.
- Dur, W., C. Simon, and J. I. Cirac, 2002, Phys. Rev. Lett. **89**, 210402.
- Eberhard, P.H., 1993, Phys. Rev. A **47**, R747.
- Eibl, M., S. Gaertner, M. Bourennane, C. Kurtsiefer, M. Zukowski, and H. Weinfurter, 2003, Phys. Rev. Lett. **90**, 200403.
- Eisenberg, H. S., G. H. Khouiry, G. A. Durkin, C. Simon, and D. Bouwmeester, 2004, Phys. Rev. Lett. **93**, 193901.
- van Enk, S. J., 2005, Phys. Rev. Lett. **95**(1), 010502.
- Escher, B.M., R.L. de Matos Filho, and L. Davidovich, 2003, Nature Phys **7**, 406.
- Fasel, S., N. Gisin, G. Ribordy, V. Scarani, and H. Zbinden, 2002, Phys. Rev. Lett. **89**(10), 107901.
- Genovese, M., 2005, Physics Reports **413**, 319.
- Ghirardi, G., 1981, Referee report to Foundation of Physics .
- Gilbert, G., and Y. S. Weinstein, 2008, J. Mod. Opt. **55**, 3283.
- Giovannetti, V., S. Lloyd, and L. Maccone, 2004, Science **306**, 1330.
- Giovannetti, V., S. Lloyd, and L. Maccone, 2006, Phys. Rev. Lett. **96**, 010401.
- Gisin, N., 1998, Physics Letters A **242**, 113.
- Gisin, N., and S. Popescu, 1999, Phys. Rev. Lett. **83**(2), 432.
- Gisin, N., G. Ribordy, W. Tittel, and H. Zbinden, 2002, Rev. Mod. Phys. **74**, 145.
- Greenberger editor, D. M. , 1986, *New Techniques and Ideas in Quantum Measurement Theory* (New York Academy of Sciences).
- Groblacher , S., K. Hammerer, M.R. Vanner, and M. Aspelmeyer, 2009, Nature **460**(), 724.
- Helstrom, C. W., 1976, *Quantum Detection and Estimation Theory* (Academic Press).
- Herbert, N., 1982, Foundation of Physics **12**, 1171.
- Hong, C. K., Z. Y. Ou, and L. Mandel, 1987, Phys. Rev. Lett. **59**, 2044.
- Horodecki, M., P. Horodecki, and R. Horodecki, 1996, Phys. Lett. A **223**, 1.
- Horodecki, R., P. Horodecki, M. Horodecki, and K. Horodecki, 2009, Rev. Mod. Phys. **81**(2), 865.
- Hubner, M., 1992, Phys. Lett. A **163**, 239.
- Huver, S., C. Wildfeuer, and J. Dowling, 2008, Phys. Rev. A **78**, 063828.
- Inouye, S., 1999, Science **285**, 517.
- Irvine, W. T. M., A. Lamas Linares, M. J. A. de Dood, and D. Bouwmeester, 2004, Phys. Rev. Lett. **92**(4), 047902.
- Jeong, H., M. Paternostro, and T. C. Ralph, 2009, Phys. Rev. Lett. **102**, 060403.
- Jozsa, R., 1994, J. Mod. Opt. **41**, 2315.
- Julsgaard, B., A. Kozhekin, and E. S. Polzik, 2001, Nature **413**, 400.
- Kacprowicz, M., R. Demkowicz-Dobrzanski, W. Wasilewski, K. Banaszek, and I. Walmsley, 2009, arXiv:0906.3511 .
- Kofler, J., and C. Brukner, 2007, Phys. Rev. Lett. **99**, 180403.
- Haroche, S., 2003, Proc. Roy. Soc. Lond. A **361**, 1339.
- Kofler, J., and C. Brukner, 2008, Phys. Rev. Lett. **101**, 090403.
- Korolkova, N., and G. Leuchs, 2002, Phys. Rev. A **71**, 032343.
- Korolkova, N., G. Leuchs, R. Loudon, T. C. Ralph, and C. Silberhorn, 2002, Phys. Rev. A **65**, 052306.
- Korsbakken, J.I., K.B. Whaley, J. Dubois, and J.I. Cirac, 2007, Phys. Rev. A **75**, 042106.
- Korsbakken, J.I., K.B. Whaley, and J.I. Cirac, 2010, Europhys. Lett. **89**, 20003.
- Kozume, 1999, Science **286**, 2309.
- Kwiat, P. G., K. Mattle, H. Weinfurter, A. Zeilinger, A. V. Sergienko, and Y. Shih, 1995a, Phys. Rev. Lett. **75**(24), 4337.
- Kwiat, P. G., K. Mattle, H. Weinfurter, A. Zeilinger, A. V. Sergienko, and Y. Shih, 1995b, Phys. Rev. Lett. **75**, 4337.
- Lamas-Linares, A., C. Simon, J. Howell, and D. Bouwmeester, 2002, Science **296**, 712.
- Lan, S.-Y., S. D. Jenkins, T. Chanelière, D. N. Matsukevich, C. J. Campbell, R. Zhao, T. A. B. Kennedy, and A. Kuzmich, 2007, Phys. Rev. Lett. **98**(12), 123602.
- Lee, S.-W., H. Jeong, and D. Jaksch, 2009, Phys. Rev. A **80**, 022104.
- Lee, C.-W., and H. Jeong, 2011, Phys. Rev. Lett. **106**, 220401.
- Leggett, A., 1980, Suppl. Prog. Theor. Phys. **69**, 80.
- Leggett, A., 2002, J. Phys. Cond. Matt. C **14**, 415.
- Leibfried, D., R. Blatt, C. Monroe, and D. Wineland, 2003, Rev. Mod. Phys. **75**(1), 281.

- Leibfried, D. e. a., 2005, *Nature (London)* **438**, 639.
- Lu, C.-Y., X.-Q. Zhou, O. Gühne, W.-B. Gao, J. Zhang, Z.-S. Yuan, A. Goebel, T. Yang, and J.-W. Pan, 2007, *Nat. Phys.* **3**, 91.
- Maccone, L., and G. De Cillis, 2009, *Phys. Rev. A* **79**, 023812.
- Mandel, L., 1983, *Nature (London)* **304**, 188.
- Marquardt, F., B. Abel, and J. von Delft, 2008, *Phys. Rev. A* **78**(), 012109.
- Markham, D., J.A. Miszczak, Z. Puchala, and K. Zyczkowski, 2008, *Phys. Rev. A* **77**(), 042111.
- Marrucci, L., 2011, *J. Optics* **13**(), 064001.
- Marshall, W., C. Simon, R. Penrose, and D. Bouwmeester, 2003, *Phys. Rev. Lett.* **91**(13), 130401.
- Massar, S., and S. Popescu, 2009, *Phys. Rev. Lett.* **74**, 1259.
- Matsukevich, D. N., T. Chanelière, S. D. Jenkins, S.-Y. Lan, T. A. B. Kennedy, and A. Kuzmich, 2006, *Phys. Rev. Lett.* **96**(3), 030405.
- Matsukevich, D. N., T. Chaneliere, M. Bhattacharya, S.-Y. Lan, S. D. Jenkins, T. A. B. Kennedy, and A. Kuzmich, 2005, *Phys. Rev. Lett.* **95**, 040405.
- Maudlin, T., 2002, *Quantum Nonlocality and Relativity* (Blackwell, Oxford).
- Milonni, P., and M. Hardies, 1982, *Physics Letters A* **92**, 321.
- Moehring, D. L., P. Maunz, S. Olmschenk, K. C. Younge, D. N. Matsukevich, L.-M. Duan, and C. Monroe, 2007, *Nature* **449**, 68.
- Mollow, B. R., and R. J. Glauber, 1967, *Phys. Rev.* **160**(5), 1076.
- Nagali, E., T. De Angelis, F. Sciarrino, and F. De Martini, 2007, *Phys. Rev. A* **76**, 042126.
- Nagali, E., D. Giovannini, L. Marrucci, S. Slussarenko, E. Santamato, and F. Sciarrino, 2010, *Phys. Rev. Lett.* **105**(7), 073602.
- Nagali, E., L. Sansoni, F. Sciarrino, F. De Martini, L. Marrucci, B. Piccirillo, E. Karimi, and E. Santamato, 2009, *Nat. Photonics* **3**(12), 720.
- Nielsen, M. A., and I. L. Chuang, 2000, *Quantum Information and Quantum Computation* (Cambridge University Press).
- Ou, Z. Y., and L. Mandel, 1988, *Phys. Rev. Lett.* **61**, 50.
- Ourjoumtsev, A., 2006, *Science* **312**(), 83.
- Ourjoumtsev, A., 2007, *Nature* **448**(), 784.
- Pan, J.-W., D. Bouwmeester, H. Weinfurter, and A. Zeilinger, 1998, *Phys. Rev. Lett.* **80**(18), 3891.
- Pan, J.-W., C. Simon, C. Brukner, and A. a. Zeilinger, 2001, *Nature* **410**, 1067.
- Pelliccia, D., V. Schettini, F. Sciarrino, C. Sias, and F. De Martini, 2003, *Phys. Rev. A* **68**, 042306.
- Peres, A., 1993, *Quantum Theory: Concepts and Methods* (Kluwer, Dordrecht).
- Peres, A., 1997, *Phys. Rev. Lett.* **77**, 1413.
- Pirandola, S., D. Vitali, P. Tombesi, and S. Lloyd, 2006, *Phys. Rev. Lett.* **97**(15), 150403.
- Portolan, S., O. Di Stefano, S. Savasta, F. Rossi, and R. Girlanda, 2006, *Phys. Rev. A* **73**(020201(R)), 020101.
- Raeisi, S., P. Sekatski, and C. Simon, 2011, *Phys. Rev. Lett.* **107**, 250401.
- Raeisi, S., W. Tittel, and C. Simon, 2011, arxiv (), 1111.7283.
- Raimond, J. M., M. Brune, and S. Haroche, 2001, *Rev. Mod. Phys.* **73**(3), 565.
- Rarity, J. G., and P. R. Tapster, 1990, *Phys. Rev. Lett.* **64**, 24952498.
- Reid, M. D., W. J. Munro, and F. De Martini, 2002, *Phys. Rev. A* **66**, 033801.
- Ricci, M., F. Sciarrino, N. J. Cerf, R. Filip, J. Fiurasek, and F. D. Martini, 2005, *Phys. Rev. Lett.* **95**, 090504.
- Ricci, M., F. Sciarrino, C. Sias, and F. De Martini, 2004, *Phys. Rev. Lett.* **92**(4), 047901.
- Rocheleau, T., 2010, *Nature* **463**(), 72.
- Rubin, M. A., and S. Kaushik, 2007, *Phys. Rev. A* **75**, 053805.
- Sanguinetti, B., E. Pomarico, P. Sekatski, H. Zbinden, and N. Gisin, 2010, *Phys. Rev. Lett.* **105**(8), 080503.
- Scarani, V., S. Iblisdir, N. Gisin, and A. Acín, 2005, *Rev. Mod. Phys.* **77**, 77.
- Schleich, W., M. Pernigo, and F. Le Kien, 1991, *Phys. Rev. A* **44**, 2172.
- Schnabel, R., W. P. Bowen, N. Treps, T. C. Ralph, H.-A. Bachor, and P. K. Lam, 2003, *Phys. Rev. A* **67**(1), 012316.
- Schrödinger, E., 1935, *Naturwissenschaften* **23**, 807.
- Sciarrino, F., and F. De Martini, 2005, *Phys. Rev. A* **72**, 062313.
- Sciarrino, F., and F. De Martini, 2007, *Phys. Rev. A* **76**, 012330.
- Sciarrino, F., C. Sias, M. Ricci, and F. De Martini, 2004a, *Physics Letters A* **323**, 34.
- Sciarrino, F., C. Sias, M. Ricci, and F. De Martini, 2004b, *Phys. Rev. A* **70**(5), 052305.
- Sciarrino, F., V. Secondi, and F. De Martini, 2006b, *Phys. Rev. A* **73**(), 40303.
- Sekatski, P., N. Brunner, C. Branciard, N. Gisin, and C. Simon, 2009, *Phys. Rev. Lett.* **103**(11), 113601.
- Sekatski, P., B. Sanguinetti, E. Pomarico, N. Gisin, and C. Simon, 2010, *Phys. Rev. A* **82**(5), 053814.
- Shaji, A., and C. M. Caves, 2007, *Phys. Rev. A* **76**, 032111.
- Shih, Y. H., and C. O. Alley, 1988, *Phys. Rev. Lett.* **61**(26), 2921.
- Shimizu, A., and T. Miyadera, 2002, *Phys. Rev. Lett.* **89**(), 270403.
- Shimizu, A., and T. Miyadera, 2005, *Phys. Rev. Lett.* **95**(), 090401.
- Simon, C., and D. Bouwmeester, 2003, *Phys. Rev. Lett.* **91**, 053601.
- Simon, C., V. Bužek, and N. Gisin, 2001, *Phys. Rev. Lett.* **87**(17), 170405.
- Simon, C., G. Weihs, and A. Zeilinger, 2000, *Phys. Rev. Lett.* **84**(13), 2993.
- Spagnolo, N., F. Sciarrino, and F. De Martini, 2010a, *Phys. Rev. A* **82**(3), 032325.
- Spagnolo, N., C. Vitelli, T. De Angelis, F. Sciarrino, and F. De Martini, 2009, *Phys. Rev. A* **80**, 032318.
- Spagnolo, N., C. Vitelli, F. Sciarrino, and F. De Martini, 2010c, *Phys. Rev. A* **82**, 052101.
- Spagnolo, N., C. Vitelli, M. Paternostro, F. Sciarrino, and F. De Martini, 2010b, *Phys. Rev. A*, **84**, **032102**.
- Stobinska, M., P. Sekatski, A. Buraczewski, N. Gisin, and G. Leuchs, 2011c, *Phys. Rev. A* **84**, 034104.
- Stobinska, M., Toppel, F., P. Sekatski, A. Buraczewski, M. Zukowski, M.V. Chekhova, G. Leuchs, and N. Gisin, 2011c, arxiv , 1108.4906.
- Teufel, J.D., 2011, *Nature* **475**(), 359.
- Vitelli, C., N. Spagnolo, F. Sciarrino, and F. De Martini, 2010a, *Phys. Rev. A* **82**(6), 062319.
- Vitelli, C., N. Spagnolo, L. Toffoli, F. Sciarrino, and F. De Martini, 2010b, *Phys. Rev. Lett.* **105**(11), 113602.
- Vitelli, C., N. Spagnolo, L. Toffoli, F. Sciarrino, and F. De Martini, 2010c, *Phys. Rev. A* **81**(3), 032123.
- Volz, J., M. Weber, D. Schlenk, W. Rosenfeld, J. Vrana, K. Saucke, C. Kurtsiefer, and H. Weinfurter, 2006, *Phys.*

- Rev. Lett. **96**(3), 030404.
- Bužek, V., and M. Hillery, 2000, Phys. Rev. A **62**(2), 022303.
- Walls, D. F., and G. J. Milburn, 1995, *Quantum Optics* (Springer).
- Weinfurter, H., and M. Żukowski, 2001, Phys. Rev. A **64**, 010102(R).
- Werner, R. F., 1989, Phys. Rev. A **40**, 4277.
- Werner, R. F., 1998, Phys. Rev. A **58**, 1827.
- Wieczorek, W., C. Schmid, N. Kiesel, R. Pohlner, O. Ghne, and H. Weinfurter, 2008, Phys. Rev. Lett. **101**, 010503.
- Wigner, E., 1932, Phys. Rev. **40**, 749.
- Wootters, W., and W. Zurek, 1982, Nature (London) **299**, 802.
- Yariv, A., 1989, *Quantum Electronics*,(Wiley)
- Żukowski, M., A. Zeilinger, M. A. Horne, and A. K. Ekert, 1993, Phys. Rev. Lett. **71**(26), 4287.
- Zhang, Z., 2011, Phys. Rev. Lett. **430**, 54
- Zhao, Z., Y.-A. Chen, A.-N. Zhang, T. Yang, H. J. Brieger, and J.-W. Pan, 2004, Nature **430**, 54
- Zurek, W. H., 2003, Rev. Mod. Phys. **75**, 715.